Journal of Medicinal Chemistry

Article

Potent, selective, water soluble, brain-permeable EP2 receptor antagonist for use in central nervous system disease models

Radhika Amaradhi, Avijit Banik, Shabber Mohammed, Vidyavathi Patro, Asheebo Rojas, Wenyi Wang, Damoder Reddy Motati, Raymond Dingledine, and Thota Ganesh

J. Med. Chem., **Just Accepted Manuscript** • DOI: 10.1021/acs.jmedchem.9b01218 • Publication Date (Web): 06 Jan 2020

Just Accepted

is published by the American Chemical Society. 1155 Sixteenth Street N.W., Washington, DC 20036

Potent, selective, water soluble, brain-permeable EP2 receptor antagonist for use in central nervous system disease models

*Radhika Amaradhi, Avijit Banik, Shabber Mohammed, Vidyavathi Patro, Asheebo Rojas, Wenyi Wang, Damoder Reddy Motati, Ray Dingledine and Thota Ganesh**

Department of Pharmacology and Chemical Biology, Emory University School of Medicine, 1510 Clifton Rd; Atlanta, GA, 30322, United States of America.

KEYWORDS: Neuroinflammation, PGE_2-receptors, Schild K_B, competitive antagonist, lead optimization, SAR, blood-brain barrier, aqueous solubility.

ABSTRACT: Activation of prostanoid EP2 receptor exacerbates neuroinflammatory and neurodegenerative pathology in central nervous system diseases such as epilepsy, Alzheimer's disease and cerebral aneurysms. A selective and brain-permeable EP2 antagonist will be useful to attenuate the inflammatory consequences of EP2 activation and to reduce the severity of these chronic diseases. We recently developed a brain-permeable EP2 antagonist **1** (TG6-10-1), which displayed anti-inflammatory and neuroprotective actions in rodent models of status epilepticus. However, this compound exhibited moderate selectivity to EP2, a short plasma half-life in rodents (1.7 h) and low aqueous solubility (27 μM), limiting its use in animal models of chronic disease. With lead optimization studies, we have developed several novel EP2 antagonists with improved water solubility, brain-penetration, high EP2 potency and selectivity. These novel inhibitors suppress inflammatory gene expression induced by EP2 receptor activation in a microglial cell line, reinforcing the use of EP2 antagonists as anti-inflammatory agents.

INTRODUCTION

Neuroinflammation has emerged as a key feature that exacerbates chronic neurodegenerative pathology in several central nervous system diseases including epilepsy, Alzheimer's disease (AD) and Parkinson's disease.[1-4] Neuroinflammation is also an early event that plays a deleterious role in status epilepticus and traumatic brain injury.[5, 6] Therefore, anti-inflammatory agents should offer a benefit to patients with these central nervous system (CNS) diseases. Production of inflammatory cytokines (interleukins) and chemokines, activation of glia, and induction of cyclooxygenase-2 are the early features of neuroinflammation.[7, 8] Thus, there is an excellent opportunity for therapeutic discovery targeting the mediators of neuroinflammatory signaling.

A significant body of evidence suggests that neuroinflammation precedes the appearance of amyloid-β plaques and neurofibrillary tangles, which themselves precede clinical signs of AD in animal models and patients.[9] Among the neuroinflammatory inducers, COX-2 has been very well studied thus far in AD patients by using small molecule inhibitors of COX-2.[10-12] Although retrospective epidemiological studies using non-selective COX-2 inhibitors suggested that chronic use of COX-2 inhibitors might prevent or delay the onset of Alzheimer's disease in patients, prospective studies concluded that selective COX-2 drugs do not provide a clear benefit for Alzheimer's patients.[13] Reconciliation of the epidemiologic studies with prospective clinical trial results might be found in the clinical trial design, in which the treatment of patients was initiated when the disease is already at advanced stages in terms of classical pathological markers β-amyloid plaques and neurofibrillary tangles, or insufficient duration of treatment. The prevailing hypothesis emerging from clinical trials of a COX-2 drug is that treatment of patients starting at the prodromal stage of disease could offer benefit, but not treatment starting at late stages of the disease. Testing this proof of concept requires administration of a drug for several months (in animals) to years (in

human) before clinical dementia symptoms are diagnosed. Regrettably, the COX-2 inhibitors cause adverse cardiovascular effects upon chronic use, by blunting PGI_2 synthesis.[14, 15] Two selective COX-2 inhibitors rofecoxib (Vioxx) and valdecoxib (Bextra) were withdrawn from the USA market, but a less selective COX-2 inhibitor, celecoxib (Celebrex), is in the clinic with black-box warning for thrombotic cardiotoxicity.[16] Thus, future anti-inflammatory therapy within the COX-2 pathway should be targeted through a specific proinflammatory prostanoid synthase or a receptor downstream of COX-2, rather than blocking the entire COX-2 signaling pathways.[17, 18]

COX-2 catalyzes the synthesis of five prostanoids, PGD_2, PGE_2, PGF_2, PGI_2 and TXA_2. These prostanoids activate nine receptors, DP1, DP2, EP1, EP2, EP3, EP4, FP, IP and TP respectively. Each of these receptors can play protective as well as deleterious roles in CNS and peripheral pathophysiologies.[17, 18] The EP2 receptor has emerged as a predominantly proinflammatory receptor that mediates much of the COX-2 driven inflammatory consequences.[19, 20] When activated by PGE_2, EP2 receptors stimulate adenylate cyclase resulting in elevation of cytoplasmic cAMP concentration, which initiates downstream events via cell signaling pathways mediated by protein kinase A or exchange protein activated by cAMP (Epac).[17, 18]

Genetic ablation of the EP2 receptor reduces oxidative damage and amyloid-β burden in a mouse model of AD.[21] EP2 deletion also attenuates neurotoxicity and reduces α-synuclein aggregation in a mouse model of PD.[22] Moreover, EP2 deletion improves motor strength and survival of the ALS mouse.[23] Furthermore, PGE_2 signaling via EP2 receptor increases injury in models of cerebral ischemia,[24] and mice lacking EP2 receptors have shown less cerebral oxidative damage produced by the activation of innate immunity.[25] EP2 activation promotes inflammation and neurotoxicity in models of status epilepticus induced by pilocarpine and diisopropylfluorophosphate (DFP).[19,

[26, 27] In vitro, microglia cultures from mice lacking EP2 have shown enhanced amyloid-β phagocytosis and are less sensitive to amyloid-β induced neurotoxicity.[28] Although these results strongly support the notion that pharmacological inhibition of EP2 should be explored in preclinical and clinical setting, the currently available EP2 antagonists have sub-optimal drug-like features such as low in vivo metabolic stability, in vivo plasma half-life and aqueous solubility for chronic dosing and proof-of-concept testing in preclinical AD models.

Initially Pfizer,[29] our laboratory [30, 31] and recently Amgen[32] identified four distinct classes of EP2 antagonists (**Figure 1A**). Only the Amgen compounds seems to be useful for chronic dosing, but the derivatives developed in Pfizer and in our laboratory displayed too low liver metabolic stability, plasma half-life, or brain permeability to be useful in chronic CNS disease models such as Alzheimer's disease. We initially identified a cinnamic amide compound TG4-155 (**Figure 1A**) from high-throughput screening as a potent EP2 antagonist.[30] Structure activity relationship study of this compound resulted in the first generation brain-permeable lead compound **1** (TG6-10-1, **Figure 1B**), which displays brain-to-plasma ratio of 1.7, but only 10-fold selectivity for EP2 over DP1, low aqueous solubility (27 μM) and moderate plasma half-life (1.7 h).[33] Thus, developing a selective, aqueous-soluble compound with enhanced plasma half-life while maintaining potency and brain permeability is the main goal of our project. In the present study, we report further lead-optimization studies that led to the synthesis of several second-generation analogs and show that improvements are made in terms of selectivity, aqueous solubility and in vivo plasma half-life. Moreover, we developed a compound **20o.HCl** (named TG11-77.HCl), which is water-soluble (2.52 mM), yet crosses the blood-brain-barrier with brain-to-plasma ratio of 0.4. Furthermore, several novel compounds in this class, including **20o.HCl** exhibited anti-inflammatory activity in EP2-expressing microglia-derived BV2 cell cultures in vitro. Therefore, compound **20o.HCl** and

other derivatives in this class are now suitable candidates for dosing into - disease models such as AD.

RESULTS AND DISCUSSION

Lead optimization studies to improve DMPK properties.

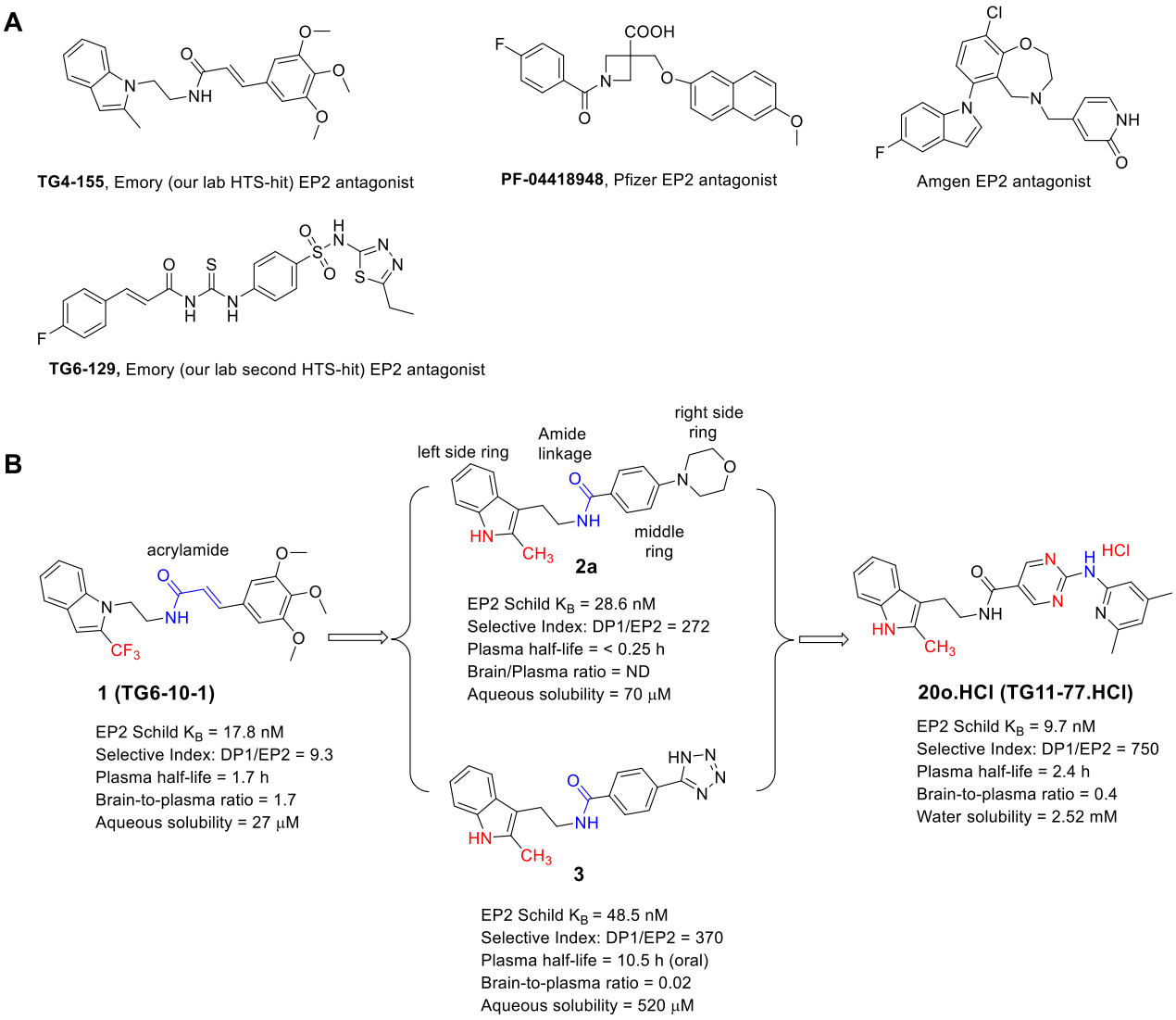

Figure 1. A. First generation EP2 antagonist hits reported in the literature. B) Lead optimization pathway identifies a brain-permeable EP2 antagonist candidate **20o.HCl** (TG11-77.HCl) from previous lead EP2 antagonist **1** (TG6-10-1)

Previous SAR studies around compound **1** (TG6-10-1, **Figure 1B**) indicated that the acrylamide moiety is not essential for EP2 bioactivity. Thus, we developed second-generation analogs with an amide linker for SAR study. Compound **2a** and **3** (**Figure 1B**) are examples of the earlier leads. These two compounds displayed high EP2 potency and selectivity and improved aqueous-solubility. However, compound **2a** displayed poor DMPK properties, for example < 2 minutes half-life in mouse liver microsomes.[34] Although compound **3** displayed excellent stability in mouse liver microsomes (> 60 min) and in vivo plasma half-life in mice (10.5 h), it showed very poor brain-to-plasma ratio of 0.02.[35] Therefore, it was not useful for proof-of concept studies in CNS disease models. The overall goal was to develop a compound with requisite brain penetration and plasma half-life. In the past, we have made several derivatives replacing the right-side ring (morpholine in **2a,** tetrazole in **3**) and learned that this ring region can be modified without substantial loss of potency at EP2 receptor. We also made limited derivatives for example, polar imidazole ring replacing the indole on the left-side ring to increase the aqueous solubility.[34] We have not made modifications on the middle phenyl ring for SAR study in the past. Therefore, we expanded our lead optimization studies with structural modification in these areas as detailed below.

Chemical synthesis

Synthesis of novel derivatives.

To explore the middle phenyl ring for structural modification and SAR studies, novel compounds **2b-c** have been synthesized in a single step (Scheme 1) using commercially available precursors (**1b** and **1c**) by following the synthetic method reported for **2a**.[34] However, several other precursors (e.g. **6a-g, 10a-c, 13a-c**) needed for synthesis of novel derivatives were not commercially

available, therefore we have synthesized here as shown in Scheme 2. Commercially available boronic acid derivatives (**4a-g**) have been coupled to 6-bromonicotinic acid (**5**) in the presence of tetrakis(triphenylphosphine)palladium (0) catalyst and a base to provide intermediates **6a-g**, which were then coupled to 2-(2-methyl-1*H*-indol-3-yl)ethan-1-amine (**7**) in the presence of 1-ethyl-3-(3-dimethylaminopropyl)carbodiimide.hydrochloride (EDCI.HCl) and (dimethylamino)pyridine (DMAP) to provide final compounds **8a-g**. Analogously, boronic acid derivatives **4a-c** on palladium catalyzed coupling with 5-bromopicolinic acid (**9**) resulted in intermediate derivatives **10a-c**, which were further coupled to **7** to provide compounds **11a-c**. Moreover, the boronic acid **4c** was coupled to 2-chloropyrimidine-5-carboxylic acid (**12a**) or 4-bromo-3-fluorobenzoic acid (**12b**) or 4-bromo-benzoic acid (**12c**) in the presence of palladium (II) catalyst and a base to result in intermediates **13a-c**, which were similarly coupled with amine **7** to furnish final compounds **14a-c**.

Scheme 1. Synthesis of middle ring modified derivatives **2b** and **2c**[a]

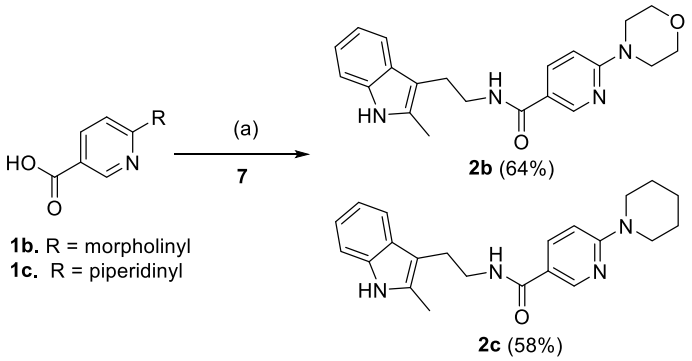

[a]*Reagents and conditions:* (a) **7** (see structure in Scheme 2), EDCI.HCl, DMAP, DMF: CH_2Cl_2 (1:1), RT, 12 h. The product yields are shown in the parenthesis

Scheme 2. Synthesis of middle ring modified EP2 antagonist derivatives[a]

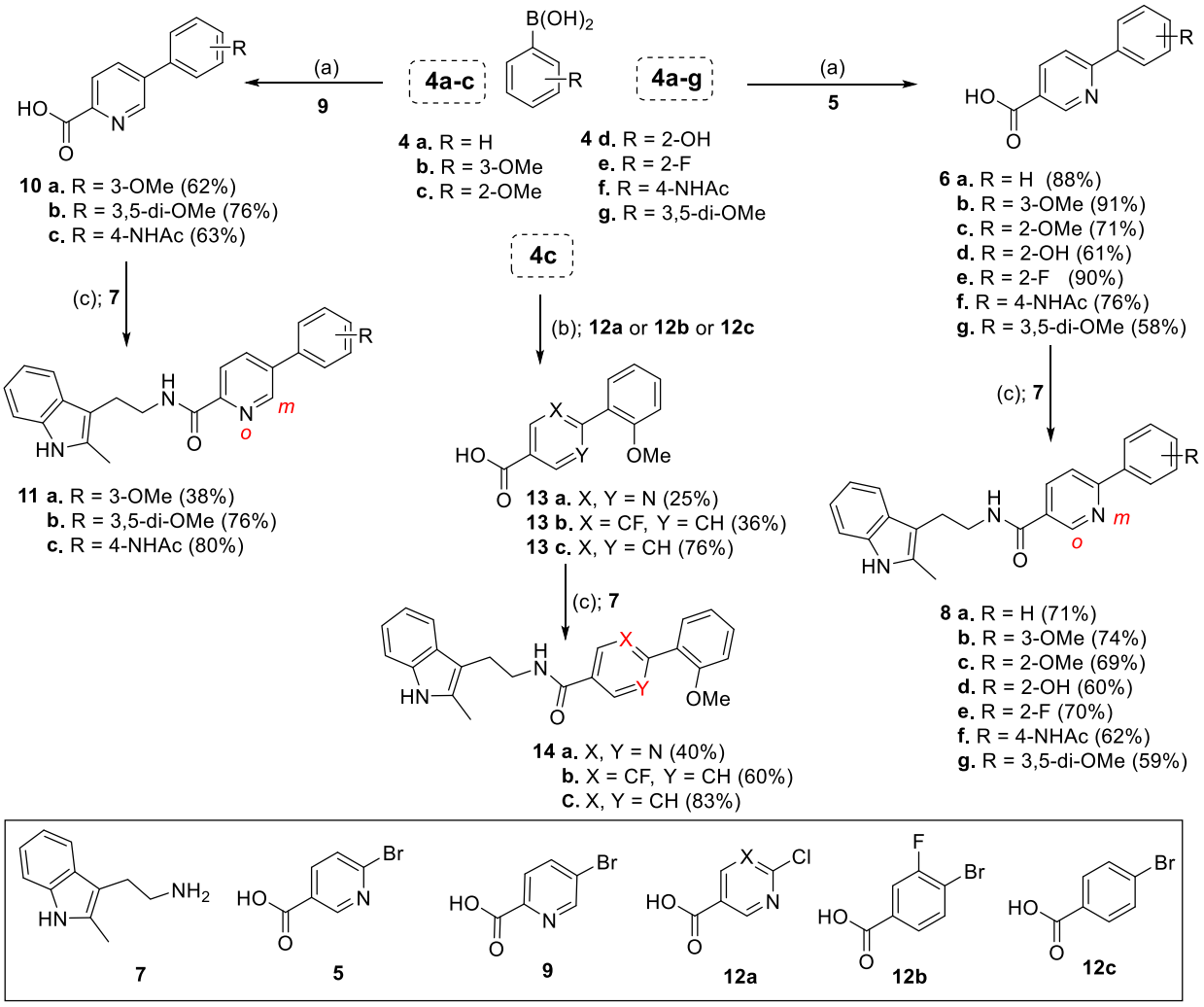

[a]*Reagents and conditions:* (a) $Pd(PPh_3)_4$, Na_2CO_3 (1M), THF (or) toluene, 100 °C, N_2; (b) $Pd(dppf)Cl_2$, dioxane:H_2O (6:1), Na_2CO_3, 100 °C; (c) EDCI.HCl, DMAP, DMF: CH_2Cl_2 (1:1), rt. Yield for each reaction product is shown in the parenthesis. Yields are isolated yields but are not optimized.

Furthermore, we synthesized a number of derivatives with 'NH' as a linking moiety between the middle ring and the last ring of the molecule. As shown in Scheme 3, the amine **7** was coupled to 2-aminopyrimidine-5-carboxylic acid (**15**) in presence of coupling reagent EDCI.HCl to provide intermediate amine **16**, which was further coupled to 2-bromopyridines **17a-o** in the presence of tris(dibenzylideneacetone)dipalladium (0) and a base to provide final products **20a-o**. Analogously, intermediate **16** was coupled to commercially available 4-bromopyridine (**18**) and

3-bromopyridines **19a-b** to provide **20p** and **20q-r** respectively as final products in good yields.

Scheme 3. Synthesis of middle and right side ring modified EP2 antagonist derivatives[a]

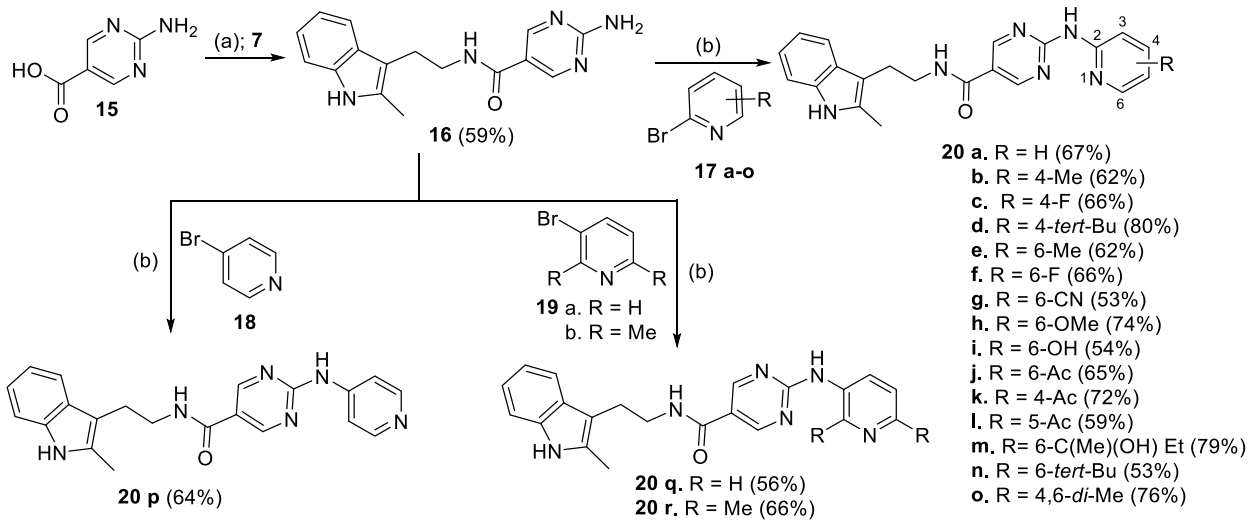

[a]*Reagents and conditions:* (a) DMAP, EDCI.HCl, DMF, rt, 24 h. (b) **17** or **18** or **19**, $Pd_2(dba)_3$, Cs_2CO_3, xantphos, dioxane, 100 °C,12-18 h; Yield for each reaction product is shown in the parenthesis.

Maintaining the middle ring as pyrimidine, and the last ring as 4,6-dimethyl pyridine (see next section for SAR discussion), we further synthesized novel compounds with substitutions on the left side indole ring. As shown in Scheme 4, ethyl-2-aminopyrimidine-5-carboxylate (**21**) on reaction with **17o** in presence of palladium (II) acetate gave intermediate **22**, which on hydrolysis afforded acid precursor **23**. Requisite amines **7a-e** (*SI* Figure 1) were synthesized using the known methods, [36,37] and they were individually coupled with **23** in the presence of DMAP and EDCI.HCl at 50 °C to furnish the final products **24a-e** (Scheme 4). Similarly, compound **24f** was synthesized using acid **23** and 2-trifluroindole-3-ethanolamine (**7f**),[38] which was intern prepared form 2-vinyl-pyrrolidin-2-one (*SI* Figure 1). Moreover, the compound 2-(2-methylpyrazolo[1,5-a]pyridin-3-yl)ethan-1-amine (**7g**) has been synthesized starting from amino-pyridinium iodide (*SI* Figure 1) .[39] Compound **7g**, and the commercially available 2-amino-1-(2-methyl-1*H*-indol-3-yl)ethan-1-

one (**7h**) and 2-amino-1-(2-methyl-1*H*-indol-3-yl)ethan-1-ol (**7i**) were coupled to the acid precursor **23** in the presence of EDCI.HCl coupling reagents to provide final products **24g-i,** respectively in moderate yields. All the intermediates and final products were characterized by complementary methods of NMR and LCMS. The compounds having purity > 95% were subjected to testing in bioassays as described below.

Scheme 4. Synthesis of left side indole and ethylene linker modified analogs[a]

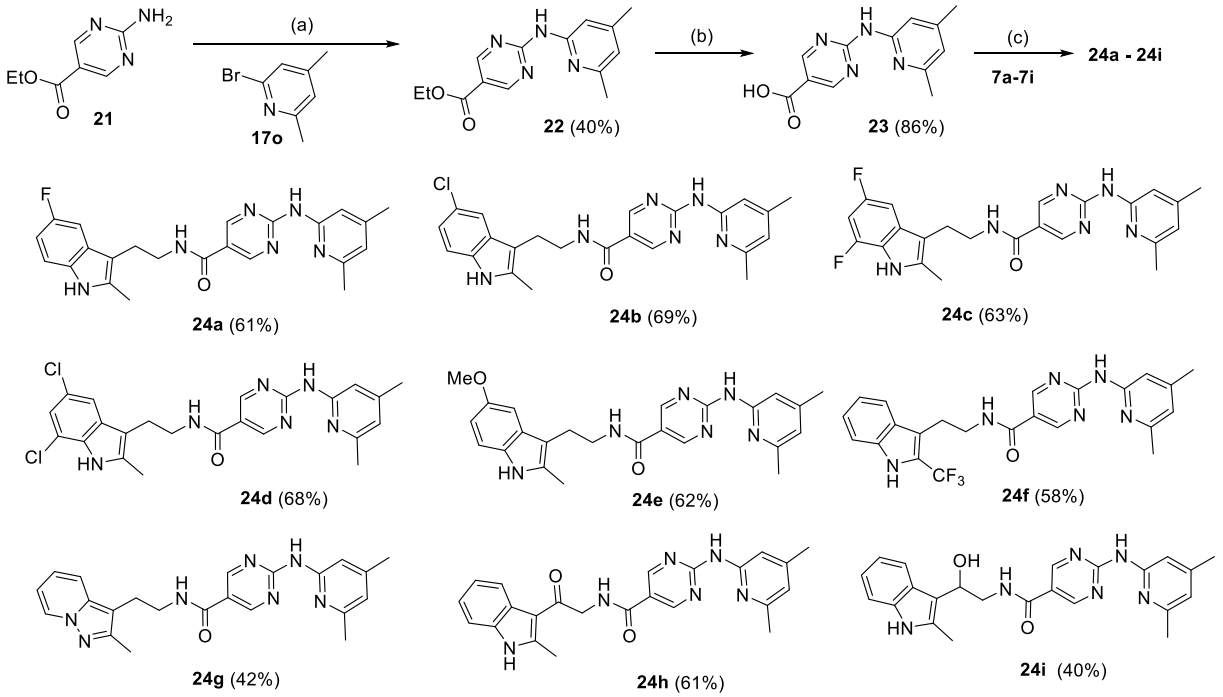

[a]*Reagents and conditions:* (a) $Pd(OAc)_2$, BINAP, Cs_2CO_3, dioxane, 100 °C, 48 h, 40%; (b) LiOH, THF:H_2O, (7:3), 12 h, 60 °C; (c) **7a-7i**, EDCI.HCl, DMAP, DMF, 50 °C, 24-48 h; Yield for each reaction product is shown in the parenthesis. Yields are isolated but not optimized.

SAR analysis of novel derivatives

Incorporation of nitrogen into the structure of small molecules often enhances aqueous solubility, intestinal permeability and other DMPK properties.[40] Therefore, we envisioned hitherto unexplored middle phenyl ring (see ring assignments in **Figure 1B**) for structural modification

with nitrogen heterocyclic rings for SAR studies. Recently, several groups have analyzed the physicochemical properties of CNS candidates and drugs to propose a multi-parameter optimization (MPO) approach that can be used to design novel chemical agents with CNS desirable properties.[41-43] Based on this MPO approach, Wager *et al.* proposed six physicochemical properties (MW, cLogP, cLogD, HBD, TPSA and pKa, Table 1) that cumulatively guide CNS activity and permeability of molecules.[43] Our previous lead compounds **2a** and **3** attained desirable MPO score (>4 out of 6 maximum), however, compound **3** was found to be a CNS impermeable compound with in vivo brain-to-plasma ratio 0.02, whereas compound **2a** was too short lived in vivo to determine the brain permeability. We also determined that **3** is not a substrate of efflux pumps, but it displayed low cell permeability P_{aap} (A-B) of 0.41 x 10^{-6} cm/sec in MDR1 expressed MDCK-cell monolayers with efflux ratio 0.3 (Table 7). Examination of its properties (Table 1) indicate that further optimization of the total polar surface area and hydrogen bond donor (HBD) properties might improve CNS permeability.[44] Moreover, compound **3** has a tetrazole ring, which is known to act as a surrogate for carboxylic acid, which could limit a passive brain permeability.[45] Therefore, we used compound **2a** as a starting point for the current lead optimization studies.

Table 1. CNS desirable properties suggested by MPO approach and calculated biophysical properties of selected EP2 antagonists including earlier leads **2a**, **3** and current lead **20o.HCl**[a]

Property	Property range for CNS drugs and candidates	**2a**	**3**	**8c**	**8g**	**14a**	**20o.HCl**
MW/FW	305-360	363	346	385	415	386	436
cLogP	2.3-3.3	3.25	2.64	4.02	3.86	3.49	3.58
cLogD (pH 7.4)	1.7-2.2	3.25	1.04	4.02	3.86	3.49	3.57

pKa	8.4	0.06	-0.65	2.28	2.83	0.59	4.5
HBD	1	2	3	2	2	2	3
PSA (Å^2)	44.8-51.2	57.36	96.4	67.0	76.2	79.9	95
MPO score	desired MPO score $\geq$ 4	**4.7**	**5.0**	**3.8**	**3.7**	**4.3**	**3.6**

[a]ChemAxon software was used to calculate the values for compounds **2a**, **3** and **20o** listed in Table 1

We previously reported compound **2a** with good EP2 potency and selectivity which showed moderate aqueous solubility.[34] It has a morpholine ring on the right, phenyl ring in the middle, and 3-indole moiety on the left side (**Figure 1B**). To learn whether the middle phenyl ring can be replaced with other rings, we synthesized and tested compound **2b** with a nicotinic acid ring. Compound **2b** displayed 4-fold less EP2 potency than **2a**, but it showed 3-fold increased aqueous solubility reinforcing the notion that nitrogen in the ring will enhance the aqueous solubility.[40] Keeping the nitrogen (nicotinic) in the middle ring, we substituted right side morpholine ring with piperidine ring (**2c**). This resulted in 6.4-fold loss of potency in comparison to **2a**. However, replacement of morpholine with a phenyl ring on the right side resulted in compound **8a**, which interestingly displayed nearly equal EP2 potency to **2a**, but low aqueous solubility (Table 2). Incorporation of a methoxy group either at 3-position (**8b**), or methoxy or hydroxy at 2-position (**8c-8d**) on the phenyl ring improved the potency by 2-fold (~10 nM, Table 2) in comparison to **2a**. Whereas, fluorine (**8e**) at 2-position reduced the potency by 2-fold in comparison to **2a**, and 4-fold in comparison to 2-methoxy derivatives **8c**. Interestingly, incorporation of 4-acetamido group (**8f**), or two methoxy groups at 3- and 5-positions (**8g**) further enhanced the potency with K_B values 4.4 and 2.9 nM respectively. To see if changing the location of nitrogen atom in the middle ring from *meta-to-ortho (*see *o-m* positional assignments in Scheme 2), we synthesized derivatives **11a-**

c. Compound **11a** was 4-fold less potent than equivalent derivative **8b**. Similarly, **11b** was 11-fold less potent than equivalent derivative **8g**, and compound **11c** was 3-fold less potent than equivalent compound **8f**. These observations suggest that nitrogen atom is preferred at *m*-position than at *o*-position of the middle ring (meaning nicotinic ring is more favorable than picolinic ring) for optimal potency. Furthermore, we synthesized a pyrimidine derivative **14a** and it showed 2.9-fold less potency than the corresponding nicotinic ring compound **8c**, but it has the same potency as initial lead **2a** in the current study. Nonetheless, nicotinic middle ring maintains high EP2 Schild potency (< 50 nM), except for **2b-c**. It is important to emphasize here that derivatives **8a-g** and **14a** displayed enhanced solubility in simulated gastric fluid at pH 2.0, whereas compounds **11a-c** have not showed solubility enhancement in the simulated gastric fluid (Table 2), suggesting nicotinic ring derivatives will have better aqueous solubility than picolinic ring derivatives. It is worth to indicate that the nitrogen in the middle ring is not absolutely essential for EP2 potency, because compound with phenyl ring, **14c** has also showed high EP2 potency (*cf.* **8c**), but a fluorine-substitution on the middle phenyl ring drastically reduced the potency by 25-fold (*cf.* **14b** vs. **14c** or **8c**) hinting that additional substitutions on the middle ring might not be tolerated for potency.

Table 2. Middle ring modified EP2 antagonists. Potency and aqueous solubility[a]

Entry	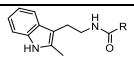 R =	EP2 K_B (nM)	Aqueous Solubility[b] (μM)	Solubility in SGF [c] (μM)
2a	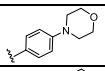	28.6	70	ND
2b	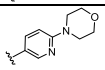	118	206	ND
2c	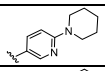	185	ND	ND
8a	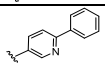	23.2	25	>100
8b	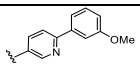	9.5	13	>100

8c	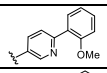	10	28	>100
8d	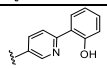	11.5	8	50[c]
8e	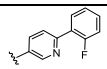	48.4	22	>100
8f	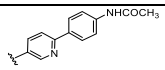	4.4	25	>100
8g	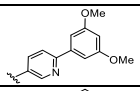	2.9	12	>100
11a	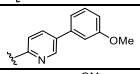	48.6	14	14
11b	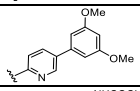	33.6	10	10
11c	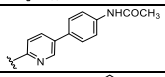	12.8	10	10
14a	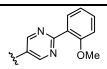	29.6	71	>100
14b	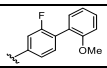	250	10	10[d]
14c	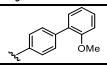	7.7	5	ND

[a]*The potency of the compounds is presented in the form of* Schild K_B values, which are calculated using the formula log (dr-1) = log X_B –log K_B, where dr (dose ratio) = fold shift in EC_{50} of PGE_2 by the antagonist compound, X_B is antagonist concentration 1 μM. K_B value indicates a concentration required to produce a 2-fold rightward shift of PGE_2 EC_{50}. K_B values are average of 2 measurements run in duplicate. [b]The solubility of the compounds is measured in PBS buffer (pH 7.4) with 1% DMSO by nephelometry.[46] [c]The numbers are derived by measuring solubility in simulated gastric fluid (SGF) at pH 2.0 with 1% DMSO by nephelometry.

Although the requisite EP2 potency is obtained for several analogs shown in Table 2, only compound **8c** has displayed good selectivity (>100-fold) against other receptors (see Table 6 and next section for selectivity discussion). Moreover, when representative compounds (**8c, 8d, 8g, 14a**) from the Table 2 were tested for stability in mouse liver microsomes, they displayed very short half-life (Table 5). Therefore, we envisioned synthesizing additional novel derivatives by keeping the middle ring as pyrimidine and modifying the third ring (Scheme 3). The other key difference between these novel set of derivatives shown in Table 3 in comparison to the ones

shown in Table 2 is the NH functional group, which links the third ring and the middle pyrimidine ring. We envisioned that the NH group should enhance the molecular flexibility and potentially allow us to make anionic salts. In the process, we first synthesized and tested 2-pyridyl derivative **20a**. Interestingly, this compound displayed high EP2 potency with K_B = 10.7 nM. Addition of methyl group (**20b**) or a fluorine (**20c**) at 4-position maintained high potency (K_B = < 10 nM). Moving the methyl group from 4- to 6- position also maintained a high potency (*cf*. **20e** vs. **20b**), but similarly moving the fluorine atom to 6- position recued the potency by 16-fold (cf. **20f** vs. **20c**). A methoxy group at 6- position also maintained high EP2 potency (**20h**), whereas cyano-group reduced the potency by 23-fold (**20g**). The acetyl group on pyridine ring whether it is at 6- ,5- or 4- position (**20j**, **20l and 20k**) reduced the potency by 4-, 20-and 12-fold respectively in comparison to **20b.** A compound with bulkier group 3-hydroxybutane at 6- position showed 4-fold less potency than **20b.** Similarly, *tert*-butyl group at 4- position reduced the potency by 5-fold (*cf.* **20d** vs. **20b**), or 6-position reduced by 13-fold (cf. **20n** vs. **20e**). A hydroxy group (**20i**) at 6-position eliminated the potency of the molecule (K_B > 1000 nM) (Table 3). Incorporation of two methyl groups as in **20o** did not have additive impact on the potency (*cf***. 20o** vs. **20b** or **20e**). We also tested the 4-pyridyl derivative **20p**, which showed complete loss of potency, whereas the 3-pyridyl derivative **20q** regained the potency and shown nearly same potency as **20a**. Addition of two methyl groups on 3-pyridyl ring (**20r**) similar to **20o** indicated 10-fold loss of potency, thus we have not subjected 3-pyridyl ring for further modification.

Table 3. Middle ring and right side ring modified EP2 antagonists. Potency and aqueous solubility[a]

Compound ID	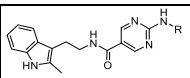 R =	EP2 K_B (nM)	Aqueous Solubility[b] (μM)
20a		10.7	27
20b		8.0	25
20c		6.4	15
20d		44.5	5
20e		6.1	25
20f		96	41
20g		230	13
20h		7.8	15
20i		1220	10
20j		32.5	5
20k		104	ND
20l		166	ND
20m		39	6
20n		79.3	25
20o		9.7	15
20p		>1000	38
20q		8.3	17
20r		88.1	100

[a]Schild K_B values are calculated similarly as indicated at Table 1 legend. K_B values are average of 2 measurements run in duplicate. ND = not determined [b]The solubility of the compounds is measured in PBS buffer (pH 7.4) with 1% DMSO by nephelometry.[46]

We then synthesized a new set of derivatives (Scheme 4) by modifying left side indole moiety and the two carbon linker, keeping the middle ring as pyrimidine and the right side ring as 4,6-dimethyl

pyridyl ring as constant. As shown in Table 4, a fluoro, chloro, methoxy, difluoro or dichloro derivatives **24a-e** all retained high EP2 potency, whereas changing indole ring to pyrazolo-pyridine ring as in **24g** reduced the potency by 32-fold in comparison to **20o**. Moreover, substituting the methyl group at second position of indole with a trifluoromethyl group (**24f**) also reduced the potency by 8-fold. Modification to the linker with ketone group next to indole (**24h**) eliminated the potency, where as a hydroxy group as in **24i** recued the potency 23-fold in comparison to **20o** suggesting unsubstituted ethylene linker is optimal for high EP2 potency within the scaffold. Overall, the SAR study on the leads indicated that a number of compounds exhibit high EP2 potency.

Table 4. Modifications at indole ring and linker regions of the scaffold. Potency and aqueous solubility[a]

Entry	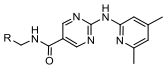 R =	EP2 K_B (nM)	Aqueous Solubility[b] (μM)	Aqueous solubility of corresponding HCl salt in SGF[c] (μM)	Water solubility of corresponding HCl salt[d] (mM)
20o		9.7	150	>250	2.52
24a		13.0	5	ND	1.16
24b		28.3	20	ND	ND
24c		20	ND	>100	1.73
24d	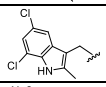	25.1	ND	ND	2.38
24e		8.8	20	ND	ND
24f		66	45	ND	0.7
24g		254	70	ND	ND

24h		>1000	ND	ND	ND
24i		183	57	ND	ND

[a]Schild K_B values are calculated similarly as indicated at Table 1 legend. K_B values are average of 2 measurements run in duplicate, except compound **20o** for which the values are average of 6 repeats [b]The solubility of the compounds is measured in PBS buffer (pH 7.4) with 1% DMSO by nephelometry.[46] [c]The solubility of compounds measured in simulated gastric fluid at pH 2.0 by nephelometry. Compound **24d** is a milky-white solution in DMSO and 24 h is an inactive compound. Therefore, their solubility is not determined by nephelometry, however, **24d.HCl** is highly water soluble. [d]Water solubility is determined by 24 h shake flask thermodynamic solubility method in neat water. Briefly, the compounds were dissolved in water at 2 mg/mL and shaken at 2200 rpm for 24 h. Then, the solutions were filtered through 0.2 μ syringe filters and analyzed the area under the curve (AUC) using HPLC, along with standard DMSO solution of each compound. ND = not determined.

Table 5. Mouse liver microsomal (MLM) stability of selected novel EP2 antagonists[a]

Compd.	MLM T1/2 (minutes)
3a	<2
8c	2.9
8d	13
8g	2.9
14a	6.5
20b	8
20c	17
20e	12
20f	96
20h	16
20o	17
24a	17
24c	26
24e	15
24i	56

[a]The compounds at 1μM were incubated in 0.125 mg/mL liver microsomes that are activated with addition of NADPH (final concentration 1 mM) and quenched the reaction at 0, 5, 15, 30, 60 and 120 min using ice-cold acetonitrile. The % compound remaining was measured using LC-MS/MS from which half-life was calculated. The work was done at CRO laboratories.

Determination of aqueous solubility of EP2 compounds

Aqueous solubility is an important property that plays crucial role in success of a drug candidate.[47] We tested several compounds for aqueous solubility by using two different methods. First, we used a kinetic assay in which we dissolved the compounds in DMSO then made serial dilutions with phosphate buffered solution (PBS) at pH 7.4, maintaining 1% DMSO in the solutions. Solubility was determined by nephelometry.[46] This assay works on the principle that when visible light is passed through a solution, part of the incident radiant energy will be scattered. The intensity of the scattered light is a function of the concentration of the dispersed phase. The nephelometric assay is used to determine either the point at which a solute begins to precipitate out of a true solution to form a suspension or the concentration at which a suspension becomes a solution when diluted further. The scattered light will remain at a constant intensity until precipitation occurs, at which point it will increase sharply. Several compounds shown in Table 2 and 3 displayed moderate solubility (< 100 μM) in PBS at pH 7.4. However, interestingly, several of those compounds including **8a-c, 8e-g, 14a**, **20o, 24c** have shown >100 μM aqueous solubility when determined in simulated gastric fluid (pH 2.0), suggesting that the intrinsic basic nitrogen can be explored to create salts that further increase solubility and facilitate the formulation. On this notion, compounds **20o, 24a, c, d** and **24f** have been converted to hydrochloride salts by stirring them in dichloromethane using dilute hydrochloride solution.

Second, to ask whether the hydrochloride salt compounds (**20o**, **24a, c d** and **24f**) are soluble in water, we used a thermodynamic assay (shake flask method)[48] where the compounds are shaken (2 mg/mL, at 2200 rpm) in neat water and the soluble fraction was measured against standard

DMSO solutions by HPLC or LC-MS/MS quantitation methods. As shown in Table 4, the hydrochloride salt compounds displayed millimolar level aqueous solubility in water. It is worth mentioning that the salt forms did not show increased solubility in PBS buffer at pH 7.4 by nephelometry method in comparison to their neutral compounds. This is likely due to a drop in pH in neat water, in comparison to a buffer. Indeed, the water pH was reduced from 6.4 to 3.5 when **20o.HCl** was dissolved at 2 mg/mL. This observation is in line with our findings that the neutral compounds have higher solubility in simulated gastric fluid (pH 2.0) than in PBS at pH 7.4. Overall, the hydrochloride salts of compounds **20o**, **24a**, **24c** and **24d** showed 2.52, 1.16, 1.73 and 2.38 mM solubility in neat water (Table 4).

Selectivity assessment of novel EP2 antagonists

The structural identity among the prostanoid receptor family is rather low. EP1, EP2, EP3 and EP4 share only 20-30% structural homology.[49] In contrast, EP2 is more homologous to DP1 (44%) and IP receptors (40%).[49] In terms of cellular signaling, EP2, EP4, DP1 and IP induce cAMP mediated cell signaling, whereas EP1 promotes Ca^{2+} mediated signaling and EP3 inhibits cAMP mediated signaling. Functionally, EP2 and DP1 receptors seem to promote inflammation in a variety of disease conditions, whereas EP4 seems to act as pro and anti-inflammatory, and the IP receptor seems to have cardioprotective role.[15] Thus, we determined the selectivity of several potent EP2 antagonists (K_B < 50 nM for EP2) against DP1 first, and if any compound showed >100-fold selectivity to DP1, then it was tested against EP4 and IP receptors. As shown in Table 6, compounds **8a-b, 8e, 11a-b** showed < 100-fold selectivity against the DP1 receptor, thus they were not tested against EP4 and IP receptors. The compounds **8c, 14a, 20a, 20c, 20e, 20h, 20o**, and **24a-c** displayed excellent selectivity against DP1, and subsequently against EP4 and IP receptors. However, compounds **8g** and **24c** displayed < 200-fold selectivity against at least one of the three

(DP1, EP4, and IP) receptors suggesting selectivity will depend on the individual structure of the molecule within the scaffold. It is worth to note that we tested several compounds in the class for cytotoxicity in the C6-glioma cell line. As exemplified in Table 6, selected compounds including **20o** displayed no cytotoxicity until 50 μM indicating > 2100-fold in vitro therapeutic index (CC_{50}/EP_2 K_B), except compound **8c** which showed CC_{50} 21 μM with a therapeutic index of 2100-fold.

Table 6. EP2 Potency, selectivity index (S.I), and cytotoxicity (CC_{50}) of selected novel EP2 antagonists[a]

Entry	EP2 K_B (nM)	DP1 K_B (μM)	S.I. (DP1/ EP2)	EP4 K_B (μM)	S.I (EP4/ EP2)	IP K_B (μM)	S.I (IP/ EP2)	CC_{50} (μM)
8a	23.2	1.0	42	ND	ND	ND	ND	ND
8b	9.5	0.9	95	ND	ND	ND	ND	ND
8c	10	3.0	300	22.8	2280	3.47	350	21
8e	48.4	0.8	16	ND	ND	ND	ND	ND
8g	2.9	1.2	410	3.91	1350	0.73	25	>50
11a	48.6	1.7	35	ND	ND	ND	ND	ND
11b	33.6	0.5	15	ND	ND	ND	ND	ND
14a	29.6	6.6	300	15.3	517	21.5	730	>50
20a	10.7	>10	>900	6.7	630	>10	>900	>50
20c	6.4	3.2	500	>10	>1500	>10	>1500	>50
20e	6.1	2.25	360	>10	>1500	>10	>1500	>50
20h	7.8	>10	>1280	6.7	860	>10	>1280	>50
20o	9.7	7.32	750	5.3	550	>10	>1000	>50
20q	8.3	1.77	213	>10	>1200	>10	>1200	>50
24a	13.0	9.0	692	3.1	240	>10	770	>50
24b	28.3	8.2	290	>10	>350	>10	>350	>50
24c	20.0	8.2	410	3.8	193	>10	>500	ND

[a]EP2 K_B values are from average of 2 independent experiments run duplicate, except for **20o**. EP4, DP1 and IP K_B values are from 2 independent experiments run in duplicate. K_B values for EP2 are in the nanomolar scale, whereas K_B values for other receptors are shown in micromolar scale. CC_{50}

(concentration required to kill 50% C6glioma cells) values are from 1-2 experiments run in triplicate using internal standard doxorubucin, which showed CC_{50} = 0.9 μM.

DMPK properties of novel EP2 antagonists

We tested several derivatives in pooled liver microsomal fractions to determine the half-life and intrinsic clearance by the mouse liver, and to project in vivo pharmacokinetics. The starting compound for the current study, **2a** was metabolized quickly in liver microsomes (Table 5). To understand the potential metabolites, we incubated compound **2a** in mouse liver microsomes and investigated metabolites after 5 minutes. As shown in Figure 2, the major metabolite is the amide bond cleaved product **D** (MW 190 Da)**,** which can be formed via intermediate **A** that would be further cleaved to generate fragments **B**/**C** (MW 158 Da) and **D**. The compound **D** can also be generated *via* a vinylamine **F** (MW 362 Da) intermediate, formation of which can be envisioned via hydroxylation at the CH_2 unit (**E**) next to 3-indole ring. Therefore, we synthesized compounds blocking the CH_2 site with a hydroxy group (e.g. **24i**). The half-life of **24i** in liver microsomes increased by 3-fold ($t_{1/2}$, 57 min) compared to its equivalent **20o**, which showed 17 minutes of half-life (Table 5). However, the hydroxylated derivatives displayed reduced EP2 potency compared with the equivalent compounds. (*cf*. **24i** displayed about 19-fold less potency than **20o**, Table 4). In a similar experiment, the tetrazole compound **3** did not produce any fragments even after 20 minutes of incubation in liver microsomes, suggesting the metabolic hydroxylation or cleavage also depends on the right side moiety (**Figure 2**). The mouse liver microsomal half-life data presented in Table 5 also indicate that a fluorine atom in place of metabolically prone methyl group enhances the stability. For example, a fluoro- derivative **20c** has 2-fold higher half-life in comparison to **20b**, like wise **20f** has 8-fold higher half-life than **20e**. Regrettably, **20c** is unstable in vivo, and **20f** displayed less potency to EP2 receptor (Table 3), therefore, these compounds are not promoted for further studies.

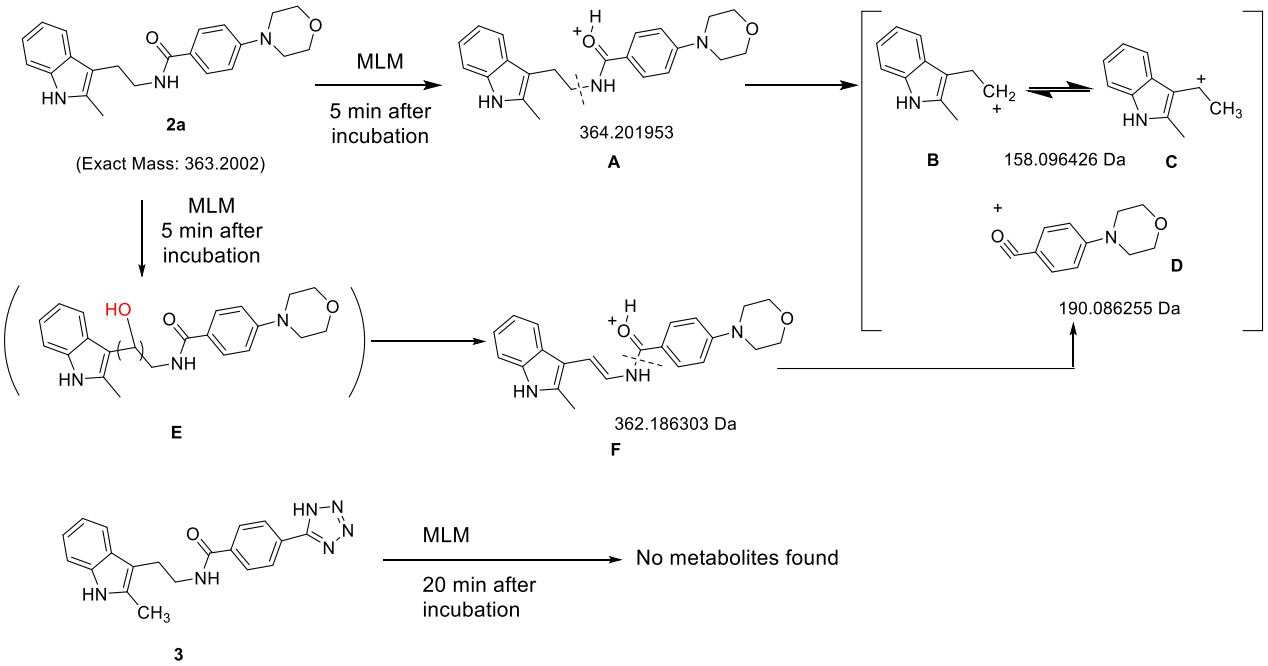

Figure 2. Metabolites identified from the lead EP2 antagonists in mouse liver microsomes.Compound **2a** was incubated for 5 min and metabolic fragments (**A-F**) were detected using LC-MS/MS. Unlike compound **2a**, compound **3** has not shown any metabolic fragments even after 20 min of incubation in mouse liver microsomes.

We estimated the CNS drug-like properties for several of these compounds before synthesis using the CNS-MPO tool.[43, 50] MPO scores indicated that several EP2 antagonists in the class as exemplified in Table 7, display a desired MPO score of $\geq$ 4, but several others do not achieve the desired score > 4 derived using their physicochemical properties. Compounds $\geq$ 4 MPO score should have desirable CNS activity and permeability features. However, the compounds **3** while it displayed > 5 score does not have good permeability properties and does not get in to the brain (Table 7). A corollary to this, the current lead compound **20o.HCl** showed < 4 MPO score, yet crosses the blood-brain-barrier with in vivo brain-to-plasma ratio 0.4. Likewise, compounds **8c, 8g** and **14a** behaved similarly. Overall, we have seen a positive correlation between MPO score to in vivo brain to plasma ratio. Nonetheless, the

MPO score does not quantitatively predict the brain permeability. We tested several compounds for permeability across MDR1 expressed MDCK cell line to investigate the potential of blood brain barrier (BBB) permeability within the class. As shown in Table 7, we found many of these compounds have good passive permeability from the apical-to-basolateral (A-B) side as well as the basolateral-to-apical side (> 0.6 x10^{-6} cm/s) in comparison to compound **3**. and their efflux ratio is < 3, except for compound **14a** which displayed ER ratio 16 indicating it may be a substrate for efflux pumps (Table 7). On the other hand, the compound **20o** found to show good permeability and showed similar efflux ratio in the presence and absence of an efflux pump inhibitor verapamil, confirming that it is not the substrate of efflux pumps. (Table 7). Moreover, compound **20o** showed 0.4 % plasma protein unbound fraction in mouse plasma proteins, but we were not able to determine its fraction unbound in the relevant brain compartment (i.e., interstitial fluid) due lack of efficient method to extract cerebrospinal fluid (CSF) from mouse brain.

Table 7. BBB-permeability, mouse and human liver microsomal stability, key pharmacokinetic properties for selected compounds[a]

Entry	MLMt $_{1/2}$(min)	HLM t $_{1/2}$ (min)	In vivo plasma t $_{1/2}$ (h)[a]	Brain-to-plasma ratio[b]	Permeability across MDR1-MDCK cell line[c]	Efflux ratio (B-A / A-B)	MPO score[d] (Desired score for CNS permeability ≥ 4)
1	10	11	1.7 (ip/po, 10 mg/kg dose)	1.7	B-A: 27.1 x 10^{-6} cm/s A-B: 25.4 x 10^{-6} cm/s	1.1	4.7
3	>60	>60	> 6h (po, 10mg/kg)	0.02	B-A: 0.12 x 10^{-6} cm/s A-B: 0.41 x 10^{-6} cm/s	0.3	5.0

8c	2.9	ND	<1h (ip, 10mg/kg)	0.5	B-A: 51.0 x 10^{-6} cm/s A-B: 19.8 x 10^{-6} cm/s	2.6	3.8
8g	2.9	ND	< 1h (ip, 10mg/kg)	ND	B-A: 55.3 x 10^{-6} cm/s A-B: 20.6 x 10^{-6} cm/s	2.7	3.7
14a	6.5	ND	< 1h (ip, 10mg/kg)	0.16	B-A: 71.1 x 10^{-6} cm/s A-B: 4.54 x 10^{-6} cm/s	16	4.3
20o	17	87.7	1.1 h (IP, 10 mg/kg) & 2.4 h (po, 50 mg/kg)	0.4	B-A: 21.5 x 10^{-6} cm/s A-B: 10.2 x 10^{-6} cm/s	2.1	3.6
In the presence of a pgp-inhibitor (verapamil)							
20o					B-A: 22.2 x 10^{-6} cm/s A-B: 13.2 x 10^{-6} cm/s	1.7	

[a]MLM = mouse liver microsomes; HLM = human liver microsomes. In liver microsomal stability tests, 1 μM compound test compound was incubated with 0.5 mg/mL liver microsomes for compounds **1** and **3**. However, other compounds in the table were incubated with 0.125 mg/mL liver microsomal concentration. The plasma half-life is estimated based on the 3-time point B/P ratio studies conducted with single injection of 10 mg/kg dose to male mice. A full-scale pharmacokinetic study with 8-time points was done for selected compounds (**1, 3, 20o**). [b]Brain-to-plasma are derived from peak concentrations observed at 0.5 h after injection in to mice. [c]BBB potential was determined using MDR1-expressed cell monolayers. All these studies are conducted at CRO laboratories following industry standard procedures. [d]See Table 1 for the physicochemical properties used to calculate the MPO score.

To determine in vivo brain-to-plasma ratio in mice, we tested several compounds whose mouse liver microsomal stability was greater than 15 min, by administering a dose of 10 mg/kg *via* intraperitoneal injection. Analysis of the compound concentration in the plasma and the brain tissues at 0.5, 2, and 4 h time points suggested that most of these compounds, exemplified as in Table 7 for **8c, 8g** & **14a**, will have a plasma half-life below 1 h, except compound **20o.** A subsequent pharmacokinetic analysis on

20o.HCl with concentration analysis at 8-time points after a single i.p. injection (10 mg/kg) (**Figure 3**) indicated that it has terminal plasma half-life 1.1 h with clearance rate of 124.1 mL/min/kg and brain-to-plasma ratio of 0.4. Additional studies with oral gavage dosing (50 mg/kg, B.I.D. dosing 8h apart) indicated that the plasma half-life could be extended to 2.4 h for **20o.HCl.**

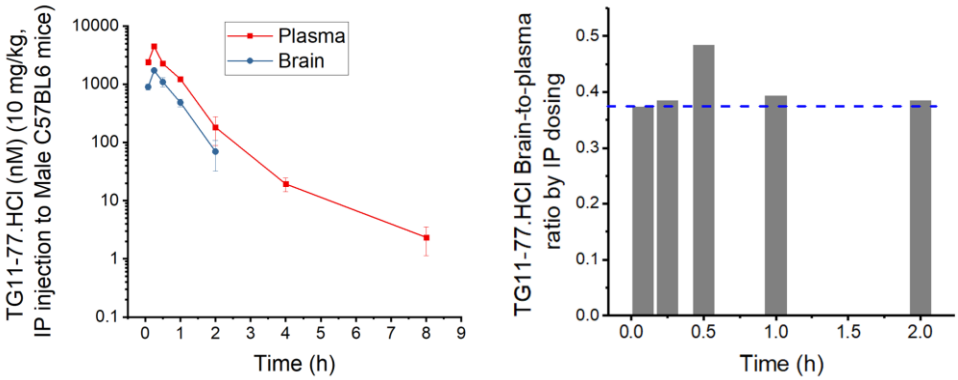

Figure 3. Pharmacokinetic parameters of **20o.HCl**. Compound **20o.HCl** was administered in to male C57BL/6 mice via intraperitoneal injection at single dose of 10 mg/kg in the vehicle of 5% NMP, 5% Solutol-HS15 and 90% water. Concentrations in plasma and brain are determined by LC-MS/MS and plotted against time.

Competitive mode of EP2 antagonism by 20o.HCl and derivatives.

To determine whether the novel derivatives in this class exhibit competitive antagonism of EP2, we tested several compounds in a concentration-response manner against PGE_2 concentration effect on EP2 receptors. *The Schild K_B indicates the antagonist concentration required for a two-fold rightward shift in the PGE_2 concentration-response curve*. Schild K_B values are derived by the equation log (dr − 1) = log X_B – log K_B, where dr = dose ratio, i.e. the fold shift in agonist EC_{50} caused by the antagonist, X_B is antagonist concentration. As illustrated in Figure 4B, a linear regression of log (dr-1) on log X_B with slope of unity characterizes a competitive antagonism. A smaller K_B value indicates a higher

inhibitory potency. As shown in Figure 4A and C, compound **20o** (TG11-77 neutral and the hydrochloride salt form) induced a concentration-dependent, parallel rightward shift in the PGE_2 concentration-response curve. Schild regression analyses (**Figure 4B**) is consistent with a competitive mechanism of antagonism on EP2 with average Schild K_B 9.7 nM and average slope value 1.05. The average K_B value is used throughout in this manuscript for discussion and comparisons. Moreover, several other compounds synthesized in this class displayed a concentration-dependent rightward shift of PGE_2 EC_{50} and with slope of unity (*SI* Figure 2). Thus, the mechanism is competitive in general for the class of EP2 antagonists presented in this study. However, compound **20o** did not show a concentration-dependent inhibition of DP1 receptor, indicating it is selective for EP2 over DP1 with selective index (DP1 K_B/EP2 K_B) of 750-fold. Moreover, this compound also showed high selectivity against EP4 and IP receptors with selective index of 550-fold and >1000-fold respectively (Table 6).

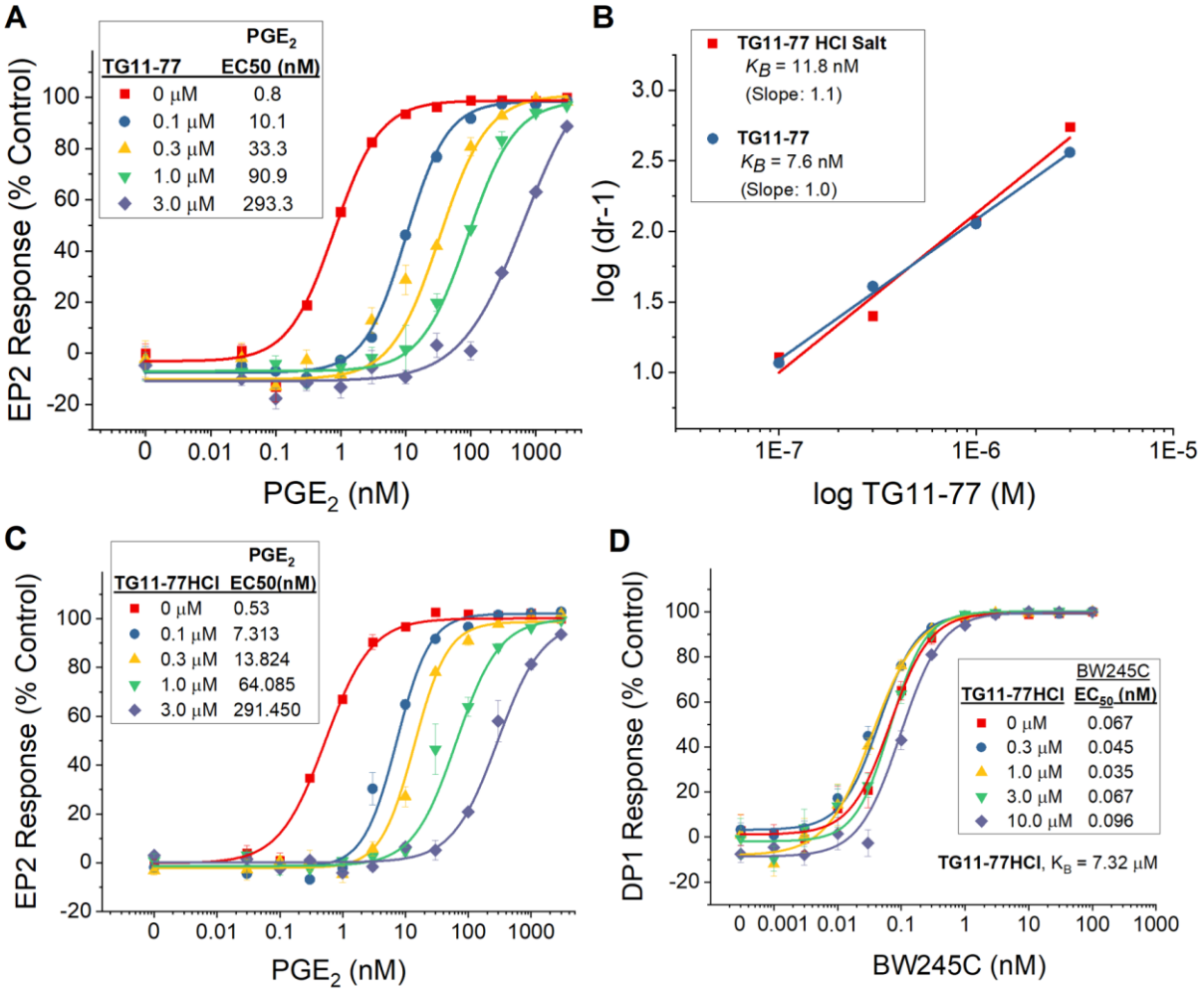

Figure 4. Competitive antagonism of EP2 receptor by **20o**. A: Compound **20o** (TG11-77 neutral) inhibited PGE_2-induced human EP2 receptor activation in a concentration dependent manner. B. Schild regression analysis is performed to determine the modality of antagonism by this compound. C. Hydrochloride salt of **20o (20o.HCl)** similarly inhibited PGE_2-induced human EP2 receptor activation in a concentration-dependent manner. Schild K_B values for neutral compound and the hydrochloride salt along with their slope values are shown in inset of Figure 4B. D. Concentration-response test of **20o.HCl** on DP1 receptors indicates it does not significantly inhibit DP1 receptor activation by agonist BW245C. Data were normalized as percentage of maximum response; points represent mean ± SEM (n = 3).

EP2 antagonists display anti-inflammatory properties in a novel microglia cell line expressing human EP2.

The EP2 receptor acts as an immunomodulator with exacerbating role in chronic neurodegenerative disease such as epilepsy and Alzheimer's disease. EP2 receptors also play an exacerbating role in chronic inflammatory diseases such as rheumatoid arthritis, inflammatory bowel disease (colitis) and endometriosis.[51-53] To determine whether the new EP2 antagonists are anti-inflammatory, we tested several of these novel EP2 antagonists including **20o** (TG11-77) for anti-inflammatory activity in vitro. A routine isolation of microglia from mouse brain proved to be low throughput and these primary cells behave variably depending on the animal. Thus, we created a hEP2-BV2 cell line, a mouse microglia cell line overexpressing human EP2 receptors.[54]. Upon activation of this cell line with 100 ng/mL lipopolysaccharide (LPS), mRNA levels of several proinflammatory genes including COX-2, IL-6 and IL-1β were induced. An EP2 specific agonist, ONO-AE1-259-01, at 30 nM further exacerbated the induction of these inflammatory genes. Gratifyingly, **20o** blunted the upregulation of inflammatory genes COX-2, IL-1β, and IL-6 in a concentration dependent manner (**Figure 5**). We found that EP2 activation in hEP2-BV2 cell line decreased mRNA levels of TNF-α consistent with the result we found with primary microglia.[55] Interestingly, these downregulated TNF-α levels are also reversed by the EP2 antagonist, reassuring that this compound is working by interacting with the EP2 receptor. In this experiment, neither the EP2 agonist (ONO-AE1-259-01), nor the antagonist (**20o**) alone showed significant effects on the expression of mRNA levels of EP2 and iNOS (an oxidative stress causing enzyme) in this cell line. Overall, these data support the use of this EP2 antagonist as an anti-inflammatory agent in inflammatory- disease models.

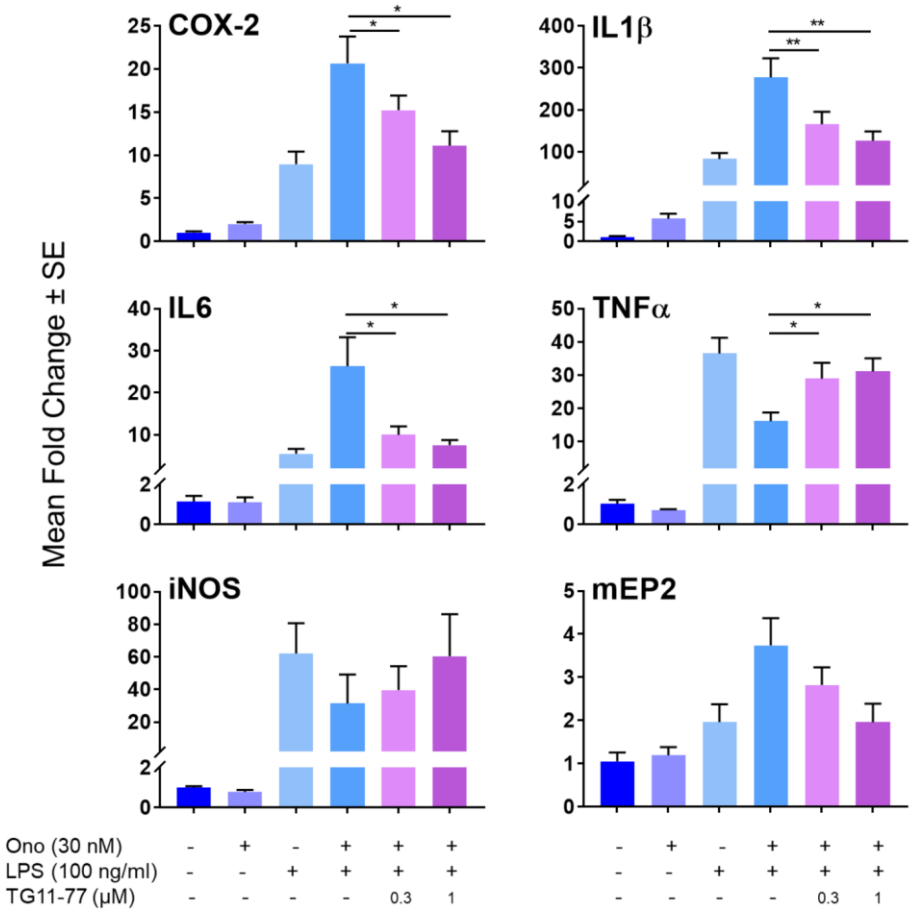

Figure 5. Mean fold change in mRNA expression of cytokines in BV2-hEP2 cells upon treatment with **20o** (TG11-77), ONO-AE1-259-01 (abbreviated as Ono in the diagram) and LPS treatment. 200,000 cells/well were grown overnight and treated with vehicle or **20o** for 1 h, vehicle or Ono for 1 h and vehicle or LPS for 2 hrs. Analyte mRNAs were measured by qRT-PCR (see *SI* Table 1 for primers used for this experiment). For statistical analysis, ΔΔCT values were used as they were normally distributed whereas fold changes were not. ANOVA-with Holm-Sidak multiple comparisons test for post-hoc analysis was used. P values were considered significant at *<0.05. Experimental repeats n = 4.

To determine whether there is a correlation between the potency of EP2 antagonists in the cAMP-production assay and their ability to inhibit inflammatory gene expression in the BV2-hEP2 cell line, we tested four selected EP2 antagonists (**3**, **20o**, **26** (TG4-155)[56] and **27** (TG8-237)[35]) with K_B values ranging between 2 and 50 nM. The fold concentrations are calculated and presented in *SI* Table 2. As shown in Figure 6, we plotted the percent inhibition of inflammatory genes against log of multiple

Schild K_B values. The results show that the inhibition of cytokines was positively correlated to their respective Schild K_B, suggesting the higher the potency of antagonists in the cAMP assay, the lower the concentration required to display maximum effect on the inflammatory genes (**Figure 6**).

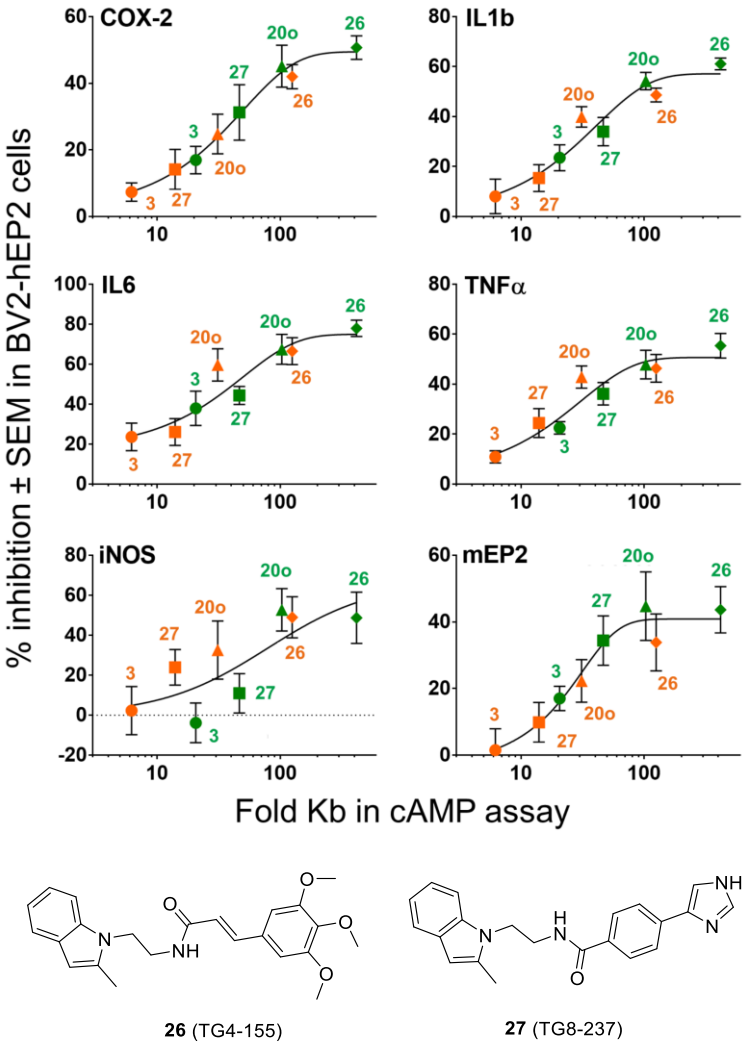

Figure 6. Concentration-related inhibition of inflammatory mediator expression by several EP2 antagonists. BV2-hEP2 microglia were incubated with combinations of the EP2 antagonists (0.3 or 1 µM), the EP2 agonist Ono (30 nM) and LPS (100 ng/ml) for 2 hours and the mRNA levels of 6 inflammatory mediators were measured. The concentrations of each antagonist on the x-axis is expressed as fold Schild K_B measured in the cAMP assay performed in C6 glioma cells overexpressing human EP2. The y-axis shows the % inhibition of the induction produced by 30 nM Ono, which is 10-fold higher than its EC50 in the cAMP assay. The data were fitted to a logistic equation. Data points are mean and SEM from 4-7 independent cultures with technical duplicates in BV2-hEP2 cells and 3-4 experimental repeats for cAMP assay in C6 glioma cells. Color coding: Orange represents data obtained with 0.3 µM of the antagonist and green represents data obtained with 1 µM.

CONCLUSIONS

In conclusion, we synthesized 45 novel EP2 antagonists with good potency and selectivity. With the lead optimization following the DMPK properties on these antagonists, a novel compound **20o.HCl** (named as TG11-77.HCl) was identified with acceptable brain permeability and excellent water solubility. Several compounds in this class displayed selective, competitive antagonism of EP2 receptors and increased solubility in simulated gastric fluid at pH 2.0 compared to PBS at pH 7.4. The hydrochloride salts of several compounds showed good water solubility at lower pH. Functionally, members of this class reversed inflammatory gene modulation by EP2 receptor activation, and the potency was shown to positively correlate to the anti-inflammatory actions measured following gene expression in a novel microglia cell line. Taken together, we conclude that **20o.HCl** should be very useful for dosing into rodent models of CNS diseases.

EXPERIMENTAL SECTION

General experimental procedures: Proton NMR spectra were recorded in solvent in DMSO-d_6/$CDCl_3$ on Varian and Inova-400 (400 MHz). Thin layer chromatography was performed on pre-coated, aluminum-backed plates (silica gel 60 F_{254}, 0.25 mm thickness) from EM Science and was visualized by UV lamp, PMA solution and ninhydrin. Chemicals and drugs: PGE_2, BW245C, iloprost, and rolipram were purchased from Cayman Chemical. LPS was purchased form Sigma-Aldrich. ONO-AE1-259-01 was generously provided by ONO Pharmaceuticals (Osaka, Japan). Column chromatography was performed with silica gel cartridges on Teledyne-ISCO instrument. Agilent LC-

MS was used to determine the mass and purity of the products. LC-MS conditions: Mobile phase A: methanol (0.1% acetic acid); mobile phase B: water (0.1% acetic acid); column: ZORBAX Eclipse XDB C18 5μM, 4.6 x 150 mm. Gradient B 80% at 0 min, linearly decreased to 5% by 7 min, and then linear increase to 40% by 12 min; UV wavelength = 254 nm; flow rate = 1 mL/min. Furthermore, purity of several key compounds is determined by Water's HPLC instrument. HPLC Conditions: Mobile phase A: water (0.1% trifluoroacetic acid); mobile phase B: acetonitrile (0.1% trifluoroacetic acid); column: XBridge C18 5μM, 4.6 x 150 mm; gradient: 10% B at 0 min, increased linearly to 90% by 10 min, then decreased to 10% by 12 min; UV wavelength = 230 nm; flow rate = 1 mL/min. Compounds with >95% purity by HPLC were tested in cellular bioassays and DMPK properties. Compounds **7a**[57], **7b**[58], **7e**[59] were reported in the literature and the characterization data for these derivatives was in good agreement with the literature data. The compound 2-(2-(trifluoromethyl)-1*H*-indol-3-yl)ethan-1-amine (**7f**) was synthesized as reported before[60, 61] and 2-(2-methylpyrazolo[1,5-a]pyridin-3-yl)ethan-1-amine (**7g**) was synthesized following the literature procedure.[62] 2-Amino-1-(2-methyl-1*H*-indol-3-yl)ethan-1-one (**7h**), and 2-amino-1-(2-methyl-1*H*-indol-3-yl)ethan-1-ol (**7i**) were commercially available.

Procedure for the synthesis of 2b and 2c:

To a solution of commercially available acid **1b** or **1c** (0.4 mmol, 1 equiv.) and **7** (70 mg, 0.4 mmol, 1 equiv.) in mixture of dichloromethane and *N,N*-dimethylformamide (3 mL, 5:1) was added DMAP (catalytic amount, 2 mg) followed by EDCI.HCl (114 mg, 0.59 mmol, 1.3 equiv.) and the reaction mixture was stirred at room temperature for 10 h. Organic solvent was evaporated and reaction mixture was added a saturated solution of ammonium chloride (5 mL) and extracted with ethyl acetate (3 x 10 mL). Organic layer was separated and washed with saturated solution of sodium bicarbonate (5 mL) followed by brine solution (5 mL), dried over sodium sulfate and concentrated to dryness. The crude

material was purified on silica gel chromatography using 60-70% ethyl acetate in hexanes to get the required product **2b** or **2c** (Scheme 1).

***N*-(2-(2-Methyl-1*H*-indol-3-yl)ethyl)-6-morpholinonicotinamide (2b)**: ^{1}H NMR (400 MHz, DMSO-d_6): δ 10.69 (s, 1H), 8.59 (d, J = 2.0 Hz, 1H), 8.40 (t, J = 5.6 Hz, 1H), 7.95 (dd, J = 8.9, 2.4 Hz, 1H), 7.44 (d, J = 7.6 Hz, 1H), 7.20 (d, J = 7.7 Hz, 1H), 6.97 – 6.85 (m, 2H), 6.81 (d, J = 9.0 Hz, 1H), 3.70 – 3.63 (m, 4H), 3.58 – 3.47 (m, 4H), 3.37 (q, J = 7.1 Hz, 2H), 2.84 (t, J = 7.4 Hz, 2H), 2.27 (s, 3H); LCMS (ESI): >97% purity. MS *m/z,* 365 $[M + H]^+$; HPLC purity: 99.7%.

***N*-(2-(2-Methyl-1*H*-indol-3-yl)ethyl)-6-(piperidin-1-yl)nicotinamide (2c):** ^{1}H NMR (400 MHz, $CDCl_3$): δ 8.36 (d, J = 2.3 Hz, 1H), 8.08 (s, 1H), 7.74 (dd, J = 9.0, 2.5 Hz, 1H), 7.51 (d, J = 7.5 Hz, 1H), 7.28 – 7.22 (m, 1H), 7.11 – 7.08 (m, 2H), 6.54 (d, J = 9.0 Hz, 1H), 6.02 (t, J = 5.6 Hz, 1H), 3.67 (q, J = 6.4 Hz, 2H), 3.57 (d, J = 5.0 Hz, 4H), 2.99 (t, J = 6.6 Hz, 2H), 2.32 (s, 3H), 1.67- 1.56 (m, 6H); LCMS (ESI): >97% purity. MS *m/z* 363 $[M + H]^+$; HPLC purity: 98.9%.

General procedure for the synthesis of 6a-g: A solution of boronic acid (**4a-g**) (4.1 mmol, 1 equiv.) and bromo-acid, **5** (4.1 mmol, 1 equiv.) in tetrahydrofuran or toluene and water (6:1) were loaded in to a sealed tube. To this solution, 1M Na_2CO_3 (8.2 mmol, 2 equiv.) was added and purged with nitrogen for 10 min. Then, $Pd(PPh_3)_4$ (0.2 mmol, 0.05 equiv.) catalyst was added to the reaction mixture, sealed and heated to 100 ^oC for 12 h. Reaction mixture was cooled to room temperature and solvent was evaporated under vacuum. The residue was washed with dichloromethane to remove organic impurities. Then, aqueous layer was acidified to pH 2 with concentrated HCl to result in white precipitate, which was filtered and dried under vacuum to provide the intermediates (**6a**, **6b**[63]**, 6c, 6d**[64]**, 6e**[65]**, 6f and 6g**).

6-Phenylnicotinic acid (6a): ^{1}H NMR (400 MHz, DMSO-d_6): δ 13.36 (s, 1H), 9.24 - 9.03 (m, 1H), 8.35 - 8.31 (m, 1H), 8.17 (dd, J = 8.2, 1.3 Hz, 2H), 8.14 - 8.09 (m, 1H), 7.54 - 7.52 (m, 3H). LCMS (ESI): >95% purity; MS *m/z*, 198 $[M - H]^+$.

6-(2-Methoxyphenyl)nicotinic acid (6c): ^{1}H NMR (300 MHz, DMSO-d_6): δ 12.52 (s, 1H), 9.14 (d, J = 2.2 Hz, 1H), 8.46 (dd, J = 8.4, 2.2 Hz, 1H), 8.11 (d, J = 8.3 Hz, 1H), 7.79 (dd, J = 7.7, 1.7 Hz, 1H), 7.59 – 7.47 (m, 1H), 7.23 (d, J = 8.2 Hz, 1H), 7.12 (dd, J = 11.5, 4.2 Hz, 1H), 3.87 (s, 3H). LCMS (ESI): >95% purity; MS *m/z*, 228 $[M - H]^+$.

6-(4-Acetamidophenyl)nicotinic acid (6f): ^{1}H NMR (300 MHz DMSO-d_6): δ 13.32 (s, 1H), 10.17 (s, 1H), 9.08 (s, 1H), 8.26 (d, J = 6.5 Hz, 1H), 8.11 (d, J = 8.6 Hz, 2H), 8.02 (d, J = 8.3 Hz, 1H), 7.72 (d, J = 8.6 Hz, 2H), 2.06 (s, 3H). LCMS (ESI): >97% purity; MS *m/z*, 255 $[M - H]^+$.

6-(3,5-Dimethoxyphenyl)nicotinic acid (6g): ^{1}H NMR (300 MHz, DMSO-d_6): δ 13.31 (bs, 1H), 9.11 (d, J = 2.2 Hz, 1H), 8.29 (dd, J = 8.3, 2.2 Hz, 1H), 8.12 (d, J = 8.4 Hz, 1H), 7.30 (d, J = 2.3 Hz, 2H), 6.61 (t, J = 2.2 Hz, 1H), 3.81 (s, 6H) . LCMS (ESI): >95% purity; MS *m/z*, 258 $[M - H]^+$.

General procedure for the synthesis of substituted 3-indole-ethylamines 7a-g: To a solution of **25a-e** (2 mmol, 1 equiv.) in acetonitrile (20 mL) was added cyclopropyl methyl ketone (4 mmol, 2 equiv.) and refluxed for 24 h. Then, reaction mixtures were cooled to room temperature. Solids precipitated were filtered to obtain corresponding hydrochloride salts of **7a-e**. To a suspension of these salts in dichloromethane was added 50% ammonium hydroxide solution (1.2 equiv.) and stirred for 3 h at room temperature. Organic layer was extracted, dried over sodium sulfate and concentrated to dryness to get the amines **7a-e** (see *SI* Figure 1). Corresponding references were provided in the general experimental section for reported compounds and data for **7c** and **7d** are shown below.

2-(5,7-Difluoro-2-methyl-1*H*-indol-3-yl)ethan-1-aminiumchloride (7c-HCl): ^{1}H NMR (400 MHz, DMSO-d_6): δ 11.48 (s, 1H), 8.15 (bs, 3H), 7.21 - 7.15 (m, 1H), 6.88 – 6.79 (m, 1H), 2.98 - 2.82 (m, 4H), 2.35 (s, 3H); LCMS (ESI): >95% purity. MS m/z, 211 [(M – HCl) + H]$^+$.

2-(5,7-Dichloro-2-methyl-1*H*-indol-3-yl)ethan-1-aminiumchloride (7d-HCl): ^{1}H NMR (400 MHz, DMSO-d_6): δ 11.46 (s, 1H), 8.13 (bs, 3H) 7.58 (s, 1H), 7.14 (s, 1H), 3.02- 2.81 (m, 4H), 2.37 (s, 3H); LCMS (ESI): >95% purity. MS m/z, 243 [(M – HCl) + H] $^+$.

General procedure for the synthesis of 8a-g: To a solution of **6a-g** (0.5 mmol, 1 equiv.) and 2-(2-methyl-1*H*-indol-3-yl)ethan-1-amine (**7**) (0.5 mmol, 1 equiv.) in *N,N*-dimethylformamide and dichloromethane (1:1) was added DMAP (catalytic amount) followed by EDCI.HCl (0.65 mmol, 1.3 equiv.) and the reaction mixture was stirred at room temperature for 10 h. Then, dichloromethane was evaporated and the crude reaction mixture was added a saturated solution of ammonium chloride (15 mL) and extracted with ethyl acetate (15 mL). Organic layer was separated and washed with saturated solution of sodium bicarbonate (15 mL) followed by brine solution (15 mL). Combined organic layer was dried over sodium sulfate, concentrated to dryness. The crude was purified on silica gel chromatography using 50-70% ethyl acetate in hexanes to get the required products (**8a-g**).

***N*-(2-(2-Methyl-1*H*-indol-3-yl)ethyl)-6-phenylnicotinamide (8a)**: ^{1}H NMR (400 MHz, $CDCl_3$): δ 8.85 (dt, J = 2.4, 0.8 Hz, 1H), 8.07 - 8.03 (m, 1H), 8.01 - 7.96 (m, 2H), 7.90 (s, 1H), 7.76 - 7.71 (m, 1H), 7.55 (d, J = 7.6 Hz, 1H), 7.51 - 7.41 (m, 3H), 7.31 (dd, J = 4.5, 4.0 Hz, 1H), 7.18 – 7.07 (m, 2H), 6.22 (t, J = 6.4 Hz, 1H), 3.76 (dd, J = 6.4, 3.4 Hz, 2H), 3.07 (t, J = 6.5 Hz, 2H), 2.40 (s, 3H); LCMS (ESI): . LCMS (ESI): >97% purity; MS *m/z*, 356 [M + H]$^+$; HPLC purity: 99.4%.

6-(3-Methoxyphenyl)-*N*-(2-(2-methyl-1*H*-indol-3-yl)ethyl)nicotinamide (8b): ^{1}H NMR (400 MHz, $CDCl_3$): δ 8.85 (dd, J = 2.3, 0.7 Hz, 1H), 8.04 (dd, J = 8.3, 2.3 Hz, 1H), 7.92 (s, 1H), 7.74 (dd, J = 8.3,

0.8 Hz, 1H), 7.60 – 7.57 (m, 1H), 7.57 – 7.53 (m, 2H), 7.39 (t, *J* = 7.9 Hz, 1H), 7.32 – 7.28 (m, 1H), 7.18 – 7.07 (m, 2H), 7.00 (dd, *J* = 8.2, 2.6 Hz, 1H), 6.23 (t, *J* = 6.0 Hz, 1H), 3.89 (s, 3H), 3.75 (dd, *J* = 6.4, 3.6 Hz, 2H), 3.07 (t, *J* = 6.5 Hz, 2H), 2.39 (s, 3H); LCMS (ESI): LCMS (ESI): >97% purity; MS *m/z*, 386 $[M + H]^+$; HPLC purity: 96.8%.

6-(2-Methoxyphenyl)-*N*-(2-(2-methyl-1*H*-indol-3-yl)ethyl)nicotinamide (8c): ^{1}H NMR (400 MHz, DMSO-d_6): δ 10.74 (s, 1H), 9.06 – 9.02 (m, 1H), 8.82 (t, *J* = 5.6 Hz, 1H), 8.19 – 8.15 (m, 1H), 7.96 – 7.92 (m, 1H), 7.81 – 7.76 (m, 1H), 7.52 – 7.40 (m, 2H), 7.25 – 7.15 (m, 2H), 7.11 – 7.05 (m, 1H), 7.01 – 6.89 (m, 2H), 3.85 (bs, 3H), 3.44 (dd, *J* = 7.4, 3.6 Hz, 2H), 2.91 (t, *J* = 7.7 Hz, 2H), 2.32 (s, 3H); LCMS (ESI): >99% purity; MS *m/z*, 386 $[M + H]^+$.

6-(2-Hydroxyphenyl)-*N*-(2-(2-methyl-1*H*-indol-3-yl)ethyl)nicotinamide (8d): ^{1}H NMR (400 MHz, DMSO-d_6): δ 13.75 (s, 1H), 10.74 (s, 1H), 9.01 (d, *J* = 1.3 Hz, 1H), 8.89 (t, *J* = 5.6 Hz, 1H), 8.39 – 8.28 (m, 2H), 8.07 (d, *J* = 8.3 Hz, 1H), 7.48 (d, *J* = 7.5 Hz, 1H), 7.35 (t, *J* = 7.7 Hz, 1H), 7.23 (d, *J* = 8.1 Hz, 1H), 7.00 – 6.89 (m, 4H), 3.49 – 3.41 (m, 2H), 2.92 (t, *J* = 7.3 Hz, 2H), 2.32 (s, 3H); LCMS (ESI): LCMS (ESI): >97% purity; MS *m/z*, 372 $[M + H]^+$; HPLC purity: 97.1%.

6-(2-Fluorophenyl)-*N*-(2-(2-methyl-1*H*-indol-3-yl)ethyl)nicotinamide (8e): ^{1}H NMR (400 MHz, $CDCl_3$): δ 8.89 (d, *J* = 1.6 Hz, 1H), 8.05 – 7.96 (m, 2H), 7.88 (s, 1H), 7.84 – 7.80 (m, 1H), 7.54 (d, *J* = 7.6 Hz, 1H), 7.44 – 7.37 (m, 1H), 7.31 – 7.25 (m, 2H), 7.19 – 7.07 (m, 3H), 6.21 (bs, 1H), 3.77 (q, *J* = 6.4 Hz, 2H), 3.07 (t, *J* = 6.5 Hz, 2H), 2.39 (s, 3H); LCMS (ESI): >99% purity; MS *m/z*, 374.0 $[M + H]^+$.

6-(4-Acetamidophenyl)-*N*-(2-(2-methyl-1*H*-indol-3-yl)ethyl)nicotinamide (8f): ^{1}H NMR (400 MHz, DMSO-d_6): δ 9.03 (d, *J* = 1.6 Hz, 1H), 8.79 (t, *J* = 5.7 Hz, 1H), 8.22 (dd, *J* = 8.4, 2.3 Hz, 1H), 8.11 (d, *J* = 8.8 Hz, 2H), 8.01 (d, *J* = 8.4 Hz, 2H), 7.73 (d, *J* = 8.7 Hz, 2H), 7.48 (d, *J* = 7.7 Hz, 1H),

7.23 (d, J = 7.6 Hz, 1H), 7.01 – 6.89 (m, 2H), 3.49 – 3.38 (m, 2H), 2.96 – 2.86 (m, 2H), 2.32 (s, 3H), 2.08 (s, 3H); LCMS (ESI): LCMS (ESI): >95% purity; *m/z*, 413 $[M + H]^+$; HPLC purity: 95.8%.

6-(3,5-Dimethoxyphenyl)-*N*-(2-(2-methyl-1*H*-indol-3-yl)ethyl)nicotinamide (8g): ^{1}H NMR (400 MHz, $CDCl_3$): δ 8.84 (s, 1H), 8.02 (dt, J = 8.3, 2.1 Hz, 1H), 7.92 (s, 1H), 7.70 (d, J = 8.3 Hz, 1H), 7.54 (d, J = 7.5 Hz, 1H), 7.30 (d, J = 7.9 Hz, 1H), 7.18 - 7.05 (m, 4H), 6.55 (q, J = 2.0 Hz, 1H), 6.23 (t, J = 4.8 Hz, 1H), 3.86 (d, J = 1.8 Hz, 6H), 3.77 (q, J = 6.3 Hz, 2H), 3.04 (t, J = 6.5 Hz, 2H), 2.39 (d, J = 1.5 Hz, 3H). LCMS (ESI): >99% purity; MS *m/z*, 416.2 $[M + H]^+$.

General procedure for the synthesis of 10a-c: A solution of boronic acid (**4a-c**) (4.1 mmol, 1 equiv.) and bromo-acid **9** (4.1 mmol, 1 equiv.) in tetrahydrofuran or toluene and water (6:1) were loaded in to a sealed tube. To this solution, 1M Na_2CO_3 (8.2 mmol, 2 equiv.) was added and purged with nitrogen for 10 min. Then, $Pd(PPh_3)_4$ (0.2 mmol, 0.05 equiv.) catalyst was added to the reaction mixture, sealed and heated to 100 ^oC for 12 h. Reaction mixture was cooled to room temperature and solvent was evaporated under vacuum. The residue was washed with dichloromethane to remove organic impurities. Then, aqueous layer was acidified to pH 2 with concentrated HCl to result in white precipitate, which was filtered and dried under vacuum to provide the intermediate**s 10a**[66]**, 10b**[66] and **10c**). Often these compounds used for next reaction without purification.

5-(4-Acetamidophenyl)picolinic acid (10c): ^{1}H NMR (400 MHz, DMSO-d_6): δ 10.18 (s, 1H), 9.01 (s, 1H), 8.24 (d, J = 11 Hz, 1H), 8.08 (d, J = 11 Hz, 1H), 7.84 – 7.70 (m, 4 H), 2.08 (s, 3H) . LCMS (ESI): >95% purity; MS *m/z*, 255 $[M - H]^+$.

General procedure for the synthesis of 11a-c: To a solution of **10a-c** (0.5 mmol, 1 equiv.) and 2-(2-methyl-1*H*-indol-3-yl)ethan-1-amine (**7**) (0.5 mmol, 1 equiv.) in *N,N*-dimethylformamide and dichloromethane (1:1) was added DMAP (catalytic amount) followed by EDCI.HCl (0.65 mmol, 1.3

equiv.) and the reaction mixture was stirred at room temperature for 10 h. Then, dichloromethane was evaporated and the crude reaction mixture was added a saturated solution of ammonium chloride (15 mL) and extracted with ethyl acetate (15 mL). Organic layer was separated and washed with saturated solution of sodium bicarbonate (15 mL) followed by brine solution (15 mL). Combined organic layer was dried over sodium sulfate, concentrated to dryness. The crude was purified on silica gel chromatography using 50-70% ethyl acetate in hexanes to get the required products (**11a-c**).

5-(3-Methoxyphenyl)-*N*-(2-(2-methyl-1*H*-indol-3-yl)ethyl)picolinamide (11a): ^{1}H NMR (400 MHz, $CDCl_3$): δ 8.68 (d, J = 2.2 Hz, 1H), 8.25 (d, J = 8.1 Hz, 1H), 8.17 (t, J = 5.6 Hz, 1H), 8.04 (s, 1H), 8.00 – 7.95 (m, 1H), 7.57 (d, J = 7.4 Hz, 1H), 7.40 (t, J = 8.0 Hz, 1H), 7.28 (d, J = 7.7 Hz, 1H), 7.18 – 7.05 (m, 4H), 6.97 (dd, J = 8.3, 2.5 Hz, 1H), 3.86 (s, 3H), 3.72 – 3.75 (m, 2H), 3.04 (t, J = 6.9 Hz, 2H), 2.37 (s, 3H); LCMS (ESI): > 98% purity; MS *m/z*, 386 $[M + H]^+$.

5-(3,5-Dimethoxyphenyl)-*N*-(2-(2-methyl-1*H*-indol-3-yl)ethyl)picolinamide (11b): ^{1}H NMR (400 MHz, $CDCl_3$): δ 8.69 (d, J = 6.8 Hz, 1H), 8.26 (d, J = 8.1 Hz, 1H), 8.16 (t, J = 5.9 Hz, 1H), 8.01 – 7.97 (m, 1H), 7.86 (s, 1H), 7.58 (d, J = 7.5 Hz, 1H), 7.31 – 7.27 (m, 1H), 7.16 – 7.06 (m, 2H), 6.71 (d, J = 2.2 Hz, 2H), 6.53 (t, J = 2.2 Hz, 1H), 3.86 (s, 6H), 3.74 (q, J = 6.8 Hz, 2H), 3.05 (t, J = 7.0 Hz, 2H), 2.39 (s, 3H); LCMS (ESI):LCMS (ESI): >97% purity; MS *m/z*, 416 $[M + H]^+$; HPLC purity: 97.6%.

5-(4-Acetamidophenyl)-*N*-(2-(2-methyl-1*H*-indol-3-yl)ethyl)picolinamide (11c): ^{1}H NMR (400 MHz, DMSO-d_6): δ 10.69 (s, 1H), 10.14 (s, 1H), 8.87 (d, J = 2.1 Hz, 1H), 8.81 (t, J = 5.9 Hz, 1H), 8.20 (dd, J = 7.4, 3.1 Hz, 1H), 8.05 (d, J = 8.1 Hz, 1H), 7.66 - 7.78 (m, 4H), 7.58 – 7.43 (m, 1H), 7.20 (d, J = 7.7 Hz, 1H), 6.96 – 6.63 (m, 2H), 3.33 – 3.46 (m, 2H), 2.88 (t, J = 7.2 Hz, 2H), 2.29 (s, 3H), 2.04 (s, 3H); LCMS (ESI): LCMS (ESI): >97% purity; MS *m/z*, 413 $[M + H]^+$.

General procedure for the synthesis 13a-c: A solution of boronic acid, **4c** (4.1 mmol, 1 equiv.) and with **12a-c** (4.1 mmol, 1 equiv.) in dioxane and water (6:1) were loaded in to a sealed tube. To this solution, 1M Na_2CO_3 (8.2 mmol, 2 equiv.) was added and purged with nitrogen for 10 min. Then, Pd(dppf)Cl_2 (0.2 mmol, 0.05 equiv.) catalyst was added to the reaction mixture, sealed and heated to 120 ºC for 12 h. Reaction mixture was cooled to room temperature and solvent was evaporated under vacuum. The residue was washed with dichloromethane to remove organic impurities. Then, aqueous layer was acidified to pH 2 with concentrated HCl to result in white precipitate, which was filtered and dried under vacuum to provide the intermediates ((**13a,**[67, 68] **13b**[69-71] and **13c**[72]).

General procedure for the synthesis of 14a-c: To a solution of **13a-c** (0.5 mmol, 1 equiv.) and 2-(2-methyl-1*H*-indol-3-yl)ethan-1-amine (**7**) (0.5 mmol, 1 equiv.) in *N,N*-dimethylformamide and dichloromethane (1:1) was added DMAP (catalytic amount) followed by EDCI.HCl (0.65 mmol, 1.3 equiv.) and the reaction mixture was stirred at room temperature for 10 h. Then, dichloromethane was evaporated and the crude reaction mixture was added a saturated solution of ammonium chloride (15 mL) and extracted with ethyl acetate (15 mL). Organic layer was separated and washed with saturated solution of sodium bicarbonate (15 mL) followed by brine solution (15 mL). Combined organic layer was dried over sodium sulfate, concentrated to dryness. The crude was purified on silica gel chromatography using 50-70% ethyl acetate in hexanes to get the required products (**14a-c**).

2-(2-Methoxyphenyl)-*N*-(2-(2-methyl-1*H*-indol-3-yl)ethyl)pyrimidine-5-carboxamide (14a): ^{1}H NMR (400 MHz, $CDCl_3$): δ 9.00 (s, 2H), 7.92 (s, 1H), 7.74 (dd, J = 7.6, 1.6 Hz, 1H), 7.53 (d, J = 7.4 Hz, 1H), 7.49 – 7.43 (m, 1H), 7.28 (d, J = 8.0 Hz, 1H), 7.17 – 6.99 (m, 4H), 6.25 (s, 1H), 3.86 (s, 3H), 3.75 (q, J = 6.4 Hz, 2H), 3.07 (t, J = 6.5 Hz, 2H), 2.37 (s, 3H); LCMS (ESI): >97% purity; MS *m/z*, 387 $[M + H]^+$.

2-Fluoro-2'-methoxy-*N*-(2-(2-methyl-1*H*-indol-3-yl)ethyl)-[1,1'-biphenyl]-4-carboxamide (14b): ^{1}H NMR (400 MHz, $CDCl_3$): δ 7.85 (s, 1H), 7.54 (d, J = 7.6 Hz, 1H), 7.44 -7.26 (m, 4H), 7.22 (d, J = 6.3 Hz, 2H), 7.17 – 7.06 (m, 2H), 7.05 – 6.95 (m, 2H), 6.16 (t, J = 5.3 Hz, 1H), 3.76 (s, 3H), 3.74 – 3.67 (m, 2H), 3.04 (t, J = 6.6 Hz, 2H), 2.38 (s, 3H); LCMS (ESI): >98% purity; MS *m/z*, 403 $[M + H]^+$.

2'-Methoxy-*N*-(2-(2-methyl-1*H*-indol-3-yl)ethyl)-[1,1'-biphenyl]-4-carboxamide (14c): ^{1}H NMR (400 MHz, DMSO-d_6): δ 10.70 (s, 1H), 8.60 (t, J = 5.9 Hz, 1H), 7.87 – 7.79 (m, 2H), 7.56 – 7.49 (m, 2H), 7.46 (d, J = 7.5 Hz, 1H), 7.37 – 7.28 (m, 2H), 7.22 – 7.17 (m, 1H), 7.11 (dd, J = 5.5, 4.6 Hz, 1H), 7.05 – 6.98 (m, 1H), 6.98 – 6.86 (m, 2H), 3.75 (d, J = 1.9 Hz, 3H), 3.43 – 3.34 (m, 2H), 2.86 (t, J = 7.4 Hz, 2H), 2.29 (d, J = 1.9 Hz, 3H); LCMS (ESI): >97% purity; MS *m/z*, 385 $[M + H]^+$; HPLC purity: 96%.

2-Amino-*N*-(2-(2-methyl-1*H*-indol-3-yl)ethyl)pyrimidine-5-carboxamide (16): To a solution of commercially available acid **15** (3 g, 21 mmol, 1 equiv.) in *N,N*-dimethylformamide (20 mL) was added DMAP (0.78 g, 6.3 mmol, 0.3 equiv.) followed by EDCI.HCl (5.35 g, 28 mmol, 1.3 equiv.) and stirred at room temperature for 10 minutes. Then, 2-(2-methyl-1*H*-indol-3-yl)ethan-1-amine (**7**) was added to the reaction mixture and stirred at room temperature for 24 h. Reaction mixture was added saturated solution of ammonium chloride (5 mL) and extracted with ethyl acetate (3 x 10 mL). Organic layer was separated and washed with saturated solution of sodium bicarbonate (5 mL) followed by brine solution. Combined organic layer was dried over sodium sulfate, concentrated to dryness. The crude material was purified on silica gel chromatography using 4-6% methanol in dichloromethane to get the required product **16** as solid (Yield: 59%). ^{1}H NMR (400 MHz, DMSO-d_6): δ 10.69 (s, 1H), 8.61 (s, 2H), 8.39 (t, J = 5.6 Hz, 1H), 7.42 (d, J = 7.7 Hz, 1H), 7.22 – 7.17 (m, 1H), 7.16 (s, 2H), 6.97 – 6.85 (m, 2H), 3.41 – 3.27 (m, 2H), 2.82 (t, J = 7.4 Hz, 2H), 2.27 (s, 3H); LCMS (ESI): > 98% purity. MS *m/z,* 296 $[M + H]^+$.

General procedure for the synthesis of 20a-20r: To a solution of **16** (0.5 mmol, 1 equiv.) and 2-bromopyridines (**17a-o or 18 or 19a-b)** (0.5 mmol, 1 equiv.) in dioxane was added Cs_2CO_3 (1.0 mmol, 2 equiv.). The solution was purged with nitrogen for 10 minutes. Then, Xantphos (0.05 mmol, 0.1 equiv.) was added followed by $Pd_2(dba)_3$ catalyst (0.05 mmol, 0.1 equiv.) and heated to 100 ^oC for 12-18 h. Reaction mixture was cooled to room temperature and added water (10 mL). Resultant solid was filtered and purified on silica gel chromatography using 3-5% methanol in dichloromethane to get the required products **20a-r**.

***N*-(2-(2-Methyl-1*H*-indol-3-yl)ethyl)-2-(pyridin-2-ylamino)pyrimidine-5-carboxamide (20a)**: ^{1}H NMR (400 MHz, DMSO-d_6): δ 10.71 (s, 1H), 10.29 (s, 1H), 8.88 (s, 2H), 8.66 (t, J = 5.4 Hz, 1H), 8.29 (d, J = 4.9 Hz, 1H), 8.21 (d, J = 8.4 Hz, 1H), 7.79 – 7.72 (m, 1H), 7.44 (d, J = 7.6 Hz, 1H), 7.20 (d, J = 7.8 Hz, 1H), 7.06 – 6.99 (m, 1H), 6.97 – 6.86 (m, 2H), 3.35- 3.42 (m, 2H), 2.86 (t, J = 7.3 Hz, 2H), 2.28 (s, 3H); LCMS (ESI): >97% purity; MS *m/z,* 373 $[M + H]^+$; HPLC purity: 98.1%.

***N*-(2-(2-Methyl-1*H*-indol-3-yl)ethyl)-2-((4-methylpyridin-2-yl)amino)pyramidine-5-carboxamide (20b)**: ^{1}H NMR (400 MHz, DMSO-d_6): δ 10.74 (s, 1H), 10.22 (s, 1H), 8.92 - 8.89 (m, 2H), 8.67 (t, J = 5.7 Hz, 1H), 8.18 (d, J = 5.0 Hz, 1H), 8.08 (s, 1H), 7.47 (d, J = 7.6 Hz, 1H), 7.26 – 7.19 (m, 1H), 7.01 – 6.87 (m, 3H), 3.45 – 3.38 (m, 2H), 2.89 (t, J = 7.3 Hz, 2H), 2.34 (s, 3H), 2.32 (s, 3H); LCMS (ESI): > 95% purity; MS *m/z,* 387 $[M + H]^+$.

2-((4-Fluoropyridin-2-yl)amino)-*N*-(2-(2-methyl-1*H*-indol-3-yl)ethyl)pyrimidine-5-carboxamide (20c): ^{1}H NMR (400 MHz, DMSO-d_6): δ 10.74 (s, 1H), 10.70 (s, 1H), 8.95 (s, 2H), 8.72 (t, J = 8 Hz 1H), 8.37 – 8.31 (m, 1H), 8.20 – 8.13 (m, 1H), 7.46 (d, J = 7.7 Hz, 1H), 7.23 (d, J = 8.0 Hz, 1H), 7.03 – 6.89 (m, 3H), 3.45- 3.38 (m, 2H), 2.89 (t, J = 6.7 Hz, 2H), 2.31 (d, J = 2.0 Hz, 3H); LCMS (ESI): >97% purity; MS *m/z,* 391 $[M + H]^+$; HPLC purity: 98.1%.

2-((4-(*tert*-Butyl)pyridin-2-yl)amino)-*N*-(2-(2-methyl-1*H*-indol-3-yl)ethyl)pyrimidine-5-carboxamide (20d): ^{1}H NMR (400 MHz, DMSO-d_6): δ 10.71 (s, 1H), 10.23 (s, 1H), 8.89 (d, J = 2.8 Hz, 2H), 8.62 (t, J = 5.6 Hz, 1H), 8.27 – 8.30 (m, 1H), 8.21 – 8.17 (m, 1H), 7.43 (d, J = 7.6 Hz, 1H), 7.20 (dd, J = 7.8, 0.8 Hz, 1H), 7.05 (dd, J = 5.3, 1.8 Hz, 1H), 6.97 – 6.85 (m, 2H), 3.42 – 3.33 (m, 2H), 2.86 (t, J = 7.3 Hz, 2H), 2.28 (s, 3H), 1.29 – 1.24 (m, 9H); LCMS (ESI): >97% purity; MS *m/z*, 429 [M + H]$^+$.

***N*-(2-(2-Methyl-1*H*-indol-3-yl)ethyl)-2-((6-methylpyridin-2-yl)amino)pyrimidine-5-carboxamide (20e)**: ^{1}H NMR (400 MHz, DMSO-d_6): δ 10.74 (s, 1H), 10.17 (s, 1H), 8.90 (d, J = 2.1 Hz, 2H), 8.67 (t, J = 5.3 Hz, 1H), 8.07 (d, J = 8.3 Hz, 1H), 7.68 (t, J = 7.8 Hz, 1H), 7.47 (d, J = 7.8 Hz, 1H), 7.23 (d, J = 7.7 Hz, 1H), 7.00 - 6.88 (m, 3H), 3.45- 3.38 (m, 2H), 2.89 (t, J = 7.4 Hz, 2H), 2.41 (s, 3H), 2.31 (s, 3H); LCMS (ESI): >98% purity; MS *m/z*, 387 [M + H]$^+$.

2-((6-Fluoropyridin-2-yl)amino)-*N*-(2-(2-methyl-1*H*-indol-3-yl)ethyl)pyrimidine-5-carboxamide (20f): ^{1}H NMR (400 MHz, DMSO-d_6): δ 10.74 (s, 1H), 10.61 (s, 1H), 8.95 – 8.91 (m, 2H), 8.73 (t, J = 5.7 Hz, 1H), 8.22 – 8.17 (m, 1H), 7.97 (q, J = 8.4 Hz, 1H), 7.47 (d, J = 7.6 Hz, 1H), 7.25 – 7.20 (m, 1H), 7.01 – 6.89 (m, 2H), 6.77 (dd, J = 7.8, 2.4 Hz, 1H), 3.45 – 3.37 (m, 2H), 2.89 (t, J = 7.4 Hz, 2H), 2.31 (s, 3H); LCMS (ESI): >97% purity. MS *m/z*, 391 [M + H]$^+$.

2-((6-Cyanopyridin-2-yl)amino)-*N*-(2-(2-methyl-1*H*-indol-3-yl)ethyl)pyrimidine-5-carboxamide (20g): ^{1}H NMR (400 MHz, DMSO-d_6): δ 10.89 (s, 1H), 10.74 (s, 1H), 8.95 (s, 2H), 8.74 (t, J = 4.8 Hz, 1H), 8.60 – 8.54 (m, 1H), 8.02 (t, J = 8.1 Hz, 1H), 7.71 – 7.61 (m, 1H), 7.46 (d, J = 7.6 Hz, 1H), 7.23 (d, J = 7.7 Hz, 1H), 7.00 - 6.89 (m, 2H), 3.42 (dd, J = 12.5, 6.2 Hz, 2H), 2.89 (t, J = 6.9 Hz, 2H), 2.31 (s, 3H); LCMS (ESI): >97% purity; MS *m/z*, 398 [M + H]$^+$; HPLC purity: 97%.

2-((6-Methoxypyridin-2-yl)amino)-*N*-(2-(2-methyl-1*H*-indol-3-yl)ethyl)pyrimidine-5-carboxamide (20h): ^{1}H NMR (400 MHz, DMSO-d_6) δ 10.74 (s, 1H), 10.07 (s, 1H), 8.91 (s, 2H), 8.68 (t, J = 5.7 Hz, 1H), 7.82 (d, J = 7.9 Hz, 1H), 7.70 (t, J = 7.9 Hz, 1H), 7.47 (d, J = 7.5 Hz, 1H), 7.23 (d, J = 7.6 Hz, 1H), 7.01 – 6.87 (m, 2H), 6.46 (d, J = 7.8 Hz, 1H), 3.85 (s, 3H), 3.45 – 3.37 (m, 2H), 2.89 (t, J = 7.1 Hz, 2H), 2.32 (s, 3H); LCMS (ESI): >96% purity; MS *m/z*, 403 $[M + H]^+$.

2-((6-Hydroxypyridin-2-yl)amino)-*N*-(2-(2-methyl-1*H*-indol-3-yl)ethyl)pyrimidine-5-carboxamide (20i): ^{1}H NMR (400 MHz, DMSO-d_6): δ 12.01 (s, 1H), 10.74 (s, 2H), 8.95 (s, 2H), 8.74 (t, J = 5.5 Hz, 1H), 7.50 – 7.40 (m, 2H), 7.23 (d, J = 8.2 Hz, 1H), 7.01 – 6.87 (m, 2H), 6.41 (bs, 1H), 5.98 (d, J = 8.8 Hz, 1H), 3.46 – 3.38 (m, 2H), 2.89 (t, J = 7.4 Hz, 2H), 2.31 (s, 3H); LCMS (ESI): >97% purity; MS *m/z*, 389 $[M + H]^+$.

2-((6-Acetylpyridin-2-yl)amino)-*N*-(2-(2-methyl-1*H*-indol-3-yl)ethyl)pyrimidine-5-carboxamide (20j): ^{1}H NMR (400 MHz, DMSO-d_6): δ 10.71 (s, 1H), 10.49 (s, 1H), 8.91 (s, 2H), 8.73 – 8.63 (m, 1H), 8.41 (d, J = 9.2 Hz, 1H), 7.96 (t, J = 7.2 Hz, 1H), 7.58 (d, J = 7.5 Hz, 1H), 7.44 (d, J = 7.2 Hz, 1H), 7.20 (d, J = 8.5 Hz, 1H), 6.98 – 6.82 (m, 2H), 3.39 (dd, J = 13.5, 6.7 Hz, 2H), 2.86 (t, J = 7.4 Hz, 2H), 2.60 (s, 3H), 2.29 (s, 3H); LCMS (ESI): >97% purity; MS *m/z*, 415 $[M + H]^+$.

2-((4-Acetylpyridin-2-yl)amino)-*N*-(2-(2-methyl-1*H*-indol-3-yl)ethyl)pyrimidine-5-carboxamide (20k): ^{1}H NMR (400 MHz, DMSO-d_6): δ 10.71 (s, 1H), 10.61 (s, 1H), 8.92 (s, 2H), 8.71 – 8.60 (m, 2H), 8.49 (d, J = 5.1 Hz, 1H), 7.54 – 7.37 (m, 2H), 7.20 (d, J = 7.7 Hz, 1H), 6.92 (dd, J , 14.1, 7.1 Hz, 2H), 3.39 (dd, J = 13.9, 6.5 Hz, 2H), 2.86 (t, J = 7.5 Hz, 2H), 2.60 (s, 3H), 2.29 (s, 3H); LCMS (ESI): >97% purity; MS *m/z*, 415 $[M + H]^+$; HPLC purity: 96.2%.

2-((5-Acetylpyridin-2-yl)amino)-*N*-(2-(2-methyl-1*H*-indol-3-yl)ethyl)pyrimidine-5-carboxamide (20l): ^{1}H NMR (400 MHz, DMSO-d_6): δ 10.87 (s, 1H), 10.72 (s, 1H), 8.94 (s, 2H), 8.88 (d, J = 2.4 Hz,

1H), 8.72 (t, *J* = 5.7 Hz, 1H), 8.38 (d, *J* = 8.9 Hz, 1H), 8.27 (dd, *J* = 8.9, 2.3 Hz, 1H), 7.44 (d, *J* = 7.5 Hz, 1H), 7.20 (d, *J* = 7.5 Hz, 1H), 6.92 (dt, *J* = 14.6, 7.0 Hz, 2H), 3.39 (dd, *J* = 13.4, 6.6 Hz, 2H), 2.87 (t, *J* = 7.3 Hz, 2H), 2.54 (s, 3H), 2.29 (s, 3H); LCMS (ESI): >98% purity; MS *m/z*, 415 $[M + H]^+$.

2-((6-(2-Hydroxybutan-2-yl)pyridin-2-yl)amino)-*N*-(2-(2-methyl-1*H*-indol-3-yl)ethyl) pyrimidine-5-carboxamide (20m): ^{1}H NMR (400 MHz, DMSO-d_6): δ 10.71 (s, 1H), 10.06 (s, 1H), 8.88 (s, 2H), 8.65 (*t*, *J* = 5.7 Hz, 1H), 8.03 (d, *J* = 8.2 Hz, 1H), 7.74 (t, *J* = 7.9 Hz, 1H), 7.43 (d, *J* = 7.6 Hz, 1H), 7.20 (dd, *J* = 7.7, 3.2 Hz, 2H), 6.91 (ddd, *J* = 14.7, 13.6, 6.2 Hz, 2H), 5.07 (s, 1H), 3.38 (dd, *J* = 13.5, 7.0 Hz, 2H), 2.86 (t, *J* = 7.3 Hz, 2H), 2.28 (s, 3H), 1.87 – 1.58 (m, 2H), 1.37 (s, 3H), 0.64 (t, *J* = 7.4 Hz, 3H); LCMS (ESI): >98% purity; MS *m/z*, 445 $[M + H]^+$.

2-((6-(*tert*-Butyl)pyridin-2-yl)amino)-*N*-(2-(2-methyl-1*H*-indol-3-yl)ethyl)pyrimidine-5-carboxamide (20n): ^{1}H NMR (400 MHz, DMSO-d_6): δ 10.71 (s, 1H), 9.87 (s, 1H), 8.88 (d, *J* = 6.0 Hz, 2H), 8.64 (t, *J* = 5.6 Hz, 1H), 7.98 (d, *J* = 8.1 Hz, 1H), 7.68 (t, *J* = 7.9 Hz, 1H), 7.44 (d, *J* = 7.3 Hz, 1H), 7.20 (d, *J* = 7.3 Hz, 1H), 7.04 (d, *J* = 7.6 Hz, 1H), 7.02 – 6.80 (m, 2H), 3.43 - 3.34 (m, 2H), 2.86 (t, *J* = 7.2 Hz, 2H), 2.29 (s, 3H), 1.30 - 1.25 (m, 9H); LCMS (ESI): >97% purity; MS *m/z*, 429 $[M + H]^+$.

2-((4,6-Dimethylpyridin-2-yl)amino)-*N*-(2-(2-methyl-1*H*-indol-3-yl)ethyl)pyrimidine-5-carboxamide (20o; TG11-77): ^{1}H NMR (400 MHz, DMSO-d_6): δ 10.74 (s, 1H), 10.08 (s, 1H), 8.90 (s, 2H), 8.65 (t, *J* = 5.5 Hz, 1H), 7.92 (s, 1H), 7.47 (d, *J* = 7.6 Hz, 1H), 7.23 (d, *J* = 7.8 Hz, 1H), 6.95 (dt, *J* = 20.4, 7.3 Hz, 2H), 6.76 (s, 1H), 3.45 – 3.37 (m, 2H), 2.89 (t, *J* = 7.3 Hz, 2H), 2.37 (s, 3H), 2.32 (s, 3H), 2.30 (s, 3H); LCMS (ESI): >95% purity. MS *m/z*, 401 $[M + H]^+$; HPLC purity: 96.4%.

2-((4,6-Dimethylpyridin-2-yl)amino)-*N*-(2-(2-methyl-1*H*-indol-3-yl)ethyl)pyrimidine-5-carboxamide.Hydrochloride (20o-HCl; TG11-77-HCl):

To a solution of **20o** (500 mg, 1.25 mmol, 1 equiv.) in dichloromethane (5 mL) was added 4M HCl in dioxane (0.62 mL, 2.5 mmol, 2 equiv.) at 0 °C and allowed to stir at room temperature for 12 h. The precipitated solid was filtered and washed with dichloromethane (5 mL) followed by ethyl acetate (5 mL) and dried to get the required salt, **20o.HCl** (Yield: 86%). ^{1}H NMR (400 MHz, DMSO-d_6): δ 11.95 (s, 1H), 10.79 (s, 1H), 9.13 (s, 2H), 8.99 (t, J = 5.3 Hz, 1H), 7.61 (s, 1H), 7.46 (d, J = 7.7 Hz, 1H), 7.23 (d, J = 7.7 Hz, 1H), 7.18 (s, 1H), 7.00 - 6.88 (m, 2H), 3.66 (bs, 1H), 3.44 (q, J = 6.7 Hz, 2H), 2.91 (t, J = 7.3 Hz, 2H), 2.62 (s, 3H), 2.47 (s, 3H), 2.32 (s, 3H); LCMS (ESI): >97% purity. MS *m/z*, 401 [(M – HCl) + H]$^+$; HPLC purity: 99%.

***N*-(2-(2-Methyl-1*H*-indol-3-yl)ethyl)-2-(pyridin-4-ylamino)pyrimidine-5-carboxamide (20p)**: ^{1}H NMR (400 MHz, DMSO-d_6): δ 10.78 (d, J = 2.3 Hz, 1H), 9.34 – 9.29 (m, 4H), 9.22 – 9.14 (m, 2H), 7.45 (d, J = 7.7 Hz, 1H), 7.20 (d, J = 7.9 Hz, 1H), 7.08 – 7.01 (m, 2H), 6.97 – 6.82 (m, 2H), 3.46 – 3.40 (m, 2H), 2.90 (t, J = 7.3 Hz, 2H), 2.29 (d, J = 2.0 Hz, 3H); LCMS (ESI): > 97% purity. MS *m/z*, 373 [M + H]$^+$.

***N*-(2-(2-Methyl-1*H*-indol-3-yl)ethyl)-2-(pyridin-3-ylamino)pyrimidine-5-carboxamide (20q)**: ^{1}H NMR (400 MHz, DMSO-d_6): δ 10.70 (s, 1H), 10.26 (s, 1H), 8.91 (s, 1H), 8.88 (s, 2H), 8.62 (t, J = 5.5 Hz, 1H), 8.26 – 8.18 (m, 2H), 7.46 (d, J = 7.6 Hz, 1H), 7.35 (dd, J = 8.2, 4.8 Hz, 1H), 7.22 (d, J = 7.8 Hz, 1H), 7.00 – 6.87 (m, 2H), 3.48 – 3.35 (m, 2H), 2.89 (t, J = 7.3 Hz, 2H), 2.32 (s, 3H); LCMS (ESI): >97% purity. MS *m/z*, 373 [M + H]$^+$; HPLC purity: 97.6%.

2-((2,6-Dimethylpyridin-3-yl)amino)-*N*-(2-(2-methyl-1*H*-indol-3-yl)ethyl)pyrimidine-5-carboxamide (20r): ^{1}H NMR (400 MHz, DMSO-d_6): δ 10.73 (s, 1H), 9.44 (s, 1H), 8.75 (s, 2H), 8.55 (t, J = 5.7 Hz, 1H), 7.64 (d, J = 8.1 Hz, 1H), 7.46 (d, J = 7.7 Hz, 1H), 7.21 (d, J = 7.6 Hz, 1H), 7.09 (d,

J = 8.1 Hz, 1H), 7.00 – 6.88 (m, 2H), 3.43 – 3.35 (m, 2H), 2.87 (t, *J* = 7.3 Hz, 2H), 2.42 (s, 3H), 2.35 (s, 3H), 2.31 (s, 3H); LCMS (ESI): >97% purity; MS *m/z*, 401[M + H]$^+$; HPLC purity: 97.3%.

Ethyl 2-((4,6-dimethylpyridin-2-yl)amino)pyrimidine-5-carboxylate (22): To a solution of **21** (250 mg, 1.6 mmol, 1 equiv.) and **17o** (35 mg, 1.6 mmol, 1 equiv.) in dioxane (5 mL) were added Cs_2CO_3 (1.1 g, 3.26 mmol, 2 equiv.) followed by BINAP (100 g, 0.16 mmol, 0.1 equiv.). Reaction mixture was purged with nitrogen for 10 minutes and added $Pd(OAc)_2$ (36 mg, 0.16 mmol, 0.1 equiv.) and heated to 100 ºC for 48 h. Reaction mixture was cooled to room temperature and added water and filtered the solid, which was purified on column chromatography using 30-40% ethyl acetate in hexanes to get the required compound **22**. ^{1}H NMR (400 MHz, $CDCl_3$): δ 11.75 (s, 1H), 9.12 (s, 2H), 8.62 (s, 1H), 6.84 (s, 1H), 4.50 – 4.28 (m, 2H), 2.70 (s, 3H), 2.54 (s, 3H), 1.40 (t, *J* = 7.1 Hz, 3H); LCMS (ESI): > 94% purity. MS *m/z*, 273 [M + H]$^+$.

2-((4,6-Dimethylpyridin-2-yl)amino)pyrimidine-5-carboxylic acid (23): To a solution of **22** (100 mg, 0.38 mmol, 1 equiv.) in tetrahydrofuran and water (7:3, 5 mL) was added $LiOH.H_2O$ (46 mg, 1.14 mmol, 3 equiv.) and heated to 60 ºC for 12 h. Reaction mixture was brought to room temperature and acidified with 1N HCl and extracted with ethyl acetate (20 mL). Organic layer was concentrated to dryness to obtain the required acid **23**. ^{1}H NMR (400 MHz, DMSO-d_6): δ 9.54 (s, 1H), 8.77 (s, 2H), 7.92 (s, 1H), 6.67 (s, 1H), 2.31 (s, 3H), 2.25 (s, 3H); LCMS (ESI): > 96% purity; MS *m/z*, 243 [M - H]$^+$.

General procedure for the synthesis of compounds 24a-i: To a solution of **23** (0.61 mmol, 1 equiv.) and compound **7a-i** (0.61 mmol, 1 equiv.) in *N,N*-dimethylformamide (5 mL) was added DMAP (catalytic amount) followed by EDCI.HCl (0.78 mmol, 1.3 equiv.) and the reaction mixture was stirred at 50 ºC for 24-48 h. Reaction mixture was brought to room temperature and added saturated solution

of ammonium chloride (10 mL) and extracted with ethyl acetate (10 mL). Organic layer was separated and washed with saturated solution of sodium bicarbonate (10 mL) followed by brine solution (10 mL). Combined organic layer was dried over sodium sulfate, concentrated to dryness. The crude was purified on silica gel chromatography using 5-7% methanol in dichloromethane to get the required products (**24a-i**).

2-((4,6-Dimethylpyridin-2-yl)amino)-*N*-(2-(5-fluoro-2-methyl-1*H*-indol-3-yl)ethyl)pyrimidine- 5-carboxamide (24a): ^{1}H NMR (400 MHz, DMSO-d_6): δ 10.85 (s, 1H), 10.06 (s, 1H), 8.88 (s, 2H), 8.63 (t, J = 5.8 Hz, 1H), 7.91 (s, 1H), 7.22 – 7.17 (m, 2H), 6.83 – 6.74 (m, 2H), 3.43 – 3.35 (m, 2H), 2.85 (t, J = 7.3 Hz, 2H), 2.36 (s, 3H), 2.31 (s, 3H), 2.29 (s, 3H); LCMS (ESI): >96% purity; MS *m/z*, 419 [M + H]$^+$.

***N*-(2-(5-Chloro-2-methyl-1*H*-indol-3-yl)ethyl)-2-((4,6-dimethylpyridin-2-yl)amino)pyrimidine-5-carboxamide (24b)**: ^{1}H NMR (400 MHz, DMSO-d_6): δ 10.97 (s, 1H), 10.09 (s, 1H), 8.89 (s, 2H), 8.63 (t, J = 4.8 Hz, 1H), 7.92 (s, 1H), 7.48 (s, 1H), 7.23 (d, J = 8.5 Hz, 1 H) 7.08 – 6.88 (m, 1H), 6.76 (s, 1H), 3.44 – 3.37 (m, 2H), 2.91 – 2.82 (m, 2H), 2.36 (s, 3H), 2.31 (s, 3H), 2.29 (s, 3H); LCMS (ESI): >95% purity; MS *m/z*, 435 [M + H]$^+$.

***N*-(2-(5,7-Difluoro-2-methyl-1*H*-indol-3-yl)ethyl)-2-((4,6-dimethylpyridin-2-yl)amino)pyrimidine-5-carboxamide (24c)**: ^{1}H NMR (400 MHz, DMSO-d_6): δ 11.32 (s, 1H), 10.09 (s, 1H), 8.88 (s, 2H), 8.62 (t, J = 5.4 Hz, 1H), 7.91 (s, 1H), 7.11 (dd, J = 9.6, 1.8 Hz, 1H), 6.82 (t, J = 10.5 Hz, 1H), 6.76 (s, 1H), 3.44 – 3.36 (m, 2H), 2.86 (t, J = 7.0 Hz, 2H), 2.37 (s, 3H), 2.32 (s, 3H), 2.29 (s, 3H); LCMS (ESI): >97% purity; MS *m/z*, 437 [M + H]$^+$.

***N*-(2-(5,7-Dichloro-2-methyl-1*H*-indol-3-yl)ethyl)-2-((4,6-dimethylpyridin-2-yl)amino)pyrimidine-5-carboxamide (24d)**: ^{1}H NMR (400 MHz, DMSO-d_6): δ 11.29 (s, 1H), 10.04

(s, 1H), 8.82 (s, 2H), 8.56 (t, *J* = 6.1 Hz, 1H), 7.92 (s, 1H), 7.45 (s, 1H), 7.09 (s, 1H), 6.73 (s, 1H), 3.36 (dd, *J* = 12.0, 5.3 Hz, 2H), 2.85 – 2.81 (m, 2H), 2.69 (s, 3H), 2.33 (s, 3H), 2.26 (s, 3H); LCMS (ESI): >95% purity; MS *m/z*, 469 $[M + H]^+$; HPLC purity: 95.5%.

2-((4,6-Dimethylpyridin-2-yl)amino)-*N*-(2-(5-methoxy-2-methyl-1*H*-indol-3-yl)ethyl)pyrimidine-5-carboxamide (24e): ^{1}H NMR (400 MHz, DMSO-d_6): δ 10.57 (s, 1H), 10.07(s, 1H), 8.89 (s, 2H), 8.64 (t, *J* = 5.6 Hz, 1H), 7.91 (s, 1H), 7.11 (d, *J* = 8.6 Hz, 1H), 6.96 (d, *J* = 2.2 Hz, 1H), 6.76 (s, 1H), 6.61 (dd, *J* = 8.6, 2.3 Hz, 1H), 3.71 (s, 3H), 3.46 – 3.35 (m, 2H), 2.85 (t, *J* = 7.2 Hz, 2H), 2.36 (s, 3H), 2.29 (bs, 6H); LCMS (ESI): >96% purity; MS *m/z*, 431 $[M + H]^+$.

2-((4,6-Dimethylpyridin-2-yl)amino)-*N*-(2-(2-(trifluoromethyl)-1*H*-indol-3-yl)ethyl)pyrimidine-5-carboxamide (24f): ^{1}H NMR (400 MHz, DMSO-d_6): δ 11.97 (s, 1H), 10.07 (s, 1H), 8.86 (bs, 2H), 8.71 (t, *J* = 5.7 Hz, 1H), 7.90 (s, 1H), 7.76 (d, *J* = 8.0 Hz, 1H), 7.44 (d, *J* = 8.3 Hz, 1H), 7.32 – 7.25 (m, 1H), 7.16 – 7.08 (m, 1H), 6.76 (s, 1H), 3.53 – 3.44 (m, 2H), 3.11 (t, *J* = 6.8 Hz, 2H), 2.36 (s, 3H), 2.29 (s, 3H); LCMS (ESI): >97% purity; MS *m/z*, 455 $[M + H]^+$.

2-((4,6-Dimethylpyridin-2-yl)amino)-*N*-(2-(2-methylpyrazolo[1,5-a]pyridin-3-yl)ethyl)pyrimidine-5-carboxamide (24g): ^{1}H NMR (400 MHz, DMSO-d_6): δ 10.03 (s, 1H), 8.81 (s, 2H), 8.59 (t, *J* = 5.6 Hz, 1H), 8.45 (dd, *J* = 7.0, 0.8 Hz, 1H), 7.86 (s, 1H), 7.47 (d, *J* = 8.8 Hz, 1H), 7.13 – 6.97 (m, 1H), 6.77 - 6.64 (m, 2H), 3.42 – 3.37 (m, 2H), 2.87 (t, *J* = 6.1 Hz, 2H), 2.33 (s, 3H), 2.30 (s, 3H), 2.25 (s, 3H); LCMS (ESI): >96% purity; MS *m/z*, 402 $[M + H]^+$.

2-((4,6-Dimethylpyridin-2-yl)amino)-*N*-(2-(2-methyl-1*H*-indol-3-yl)-2-oxoethyl)pyrimidine-5-carboxamide (24h): ^{1}H NMR (400 MHz, DMSO-d_6): δ 11.97 (s, 1H), 10.10 (s, 1H), 8.97 (s, 2H), 8.82 (t, *J* = 6.6 Hz, 1H), 8.05 – 7.95 (m, 1H), 7.91 (s, 1H), 7.46 – 7.33 (m, 1H), 7.21 – 7.10 (m, 2H), 6.74

(s, 1H), 4.72 – 4.53 (m, 2H), 2.71 (s, 3H), 2.34 (s, 3H), 2.27 (s, 3H); LCMS (ESI): >98% purity; MS *m*/z, 415 $[M + H]^+$.

2-((4,6-Dimethylpyridin-2-yl)amino)-*N*-(2-hydroxy-2-(2-methyl-1*H*-indol-3-yl)ethyl)pyrimidine-5-carboxamide (24i): ^{1}H NMR (400 MHz, DMSO-d_6): δ 10.77 (s, 1H), 10.06 (s, 1H), 8.63 (t, J = 8 Hz, 1H), 8.90 (s, 2H), 7.91 (s, 1H), 7.65 (d, J = 8 Hz, 1H), 7.26 – 7.20 (m, 1H), 7.00 – 6.88 (m, 2H), 6.76 (s, 1H), 5.21 (d, J = 3.3 Hz, 1H), 5.09 - 5.03 (t, J = 8.2 Hz, 1H), 3.66 – 3.44 (m, 2H), 2.36 (s, 3H), 2.35 (s, 3H), 2.29 (s, 3H); LCMS (ESI): >96% purity; MS *m/z*, 417 $[M + H]^+$.

Cell Culture. The rat C6 glioma (C6G) cells stably expressing human DP1, EP2, EP4, or IP receptors were created in the laboratory[19, 30, 73] and grown in Dulbecco's Modified Eagle Medium (DMEM) (Invitrogen) supplemented with 10% (v/v) fetal bovine serum (FBS) (Invitrogen), 100 U/mL penicillin, 100 µg/mL streptomycin (Invitrogen), and 0.5 µg/mL G418 (Invitrogen).

Cell-Based cAMP Assay. Intracellular cAMP was measured with a cell-based homogeneous time-resolved fluorescence resonance energy transfer (TR-FRET) method (Cisbio Bioassays), as previously described.[19, 30] The assay is based on generation of a strong FRET signal upon the interaction of two molecules, an anti-cAMP antibody coupled to a FRET donor (Cryptate) and cAMP coupled to a FRET acceptor (d2). Endogenous cAMP produced by cells competes with labeled cAMP for binding to the cAMP antibody and thus reduces the FRET signal. Cells stably expressing human DP1, EP2, EP4, or IP receptors were seeded into 384-well plates in 30 µL complete medium (4,000 cells/well) and grown overnight. The medium was carefully withdrawn and 10 µL Hanks' Buffered Salt Solution (HBSS) (Hyclone) containing 20 µM rolipram was added into the wells to block phosphodiesterases. The cells were incubated at room temperature for 0.5-1 h and then treated with vehicle or test compound for 10 min before addition of increasing concentrations of appropriate agonist: BW245C for DP1, PGE_2 for

EP2 and EP4, or iloprost for IP. The cells were incubated at room temperature for 40 min, then lysed in 10 μL lysis buffer containing the FRET acceptor cAMP-d2 and 1 min later another 10 μL lysis buffer with anti-cAMP-Cryptate was added. After 60-90 min incubation at room temperature, the FRET signal was measured by an Envision 2103 Multilabel Plate Reader (PerkinElmer Life Sciences) with a laser excitation at 337 nm and dual emissions at 665 nm and 590 nm for d2 and Cryptate (50 μs delay), respectively. The FRET signal was expressed as: $F665/F590 \times 10^4$.

Cytokine induction assay. Stable BV2-hEP2 microglia cells were created in the lab[54] and were grown overnight on poly-D-lysine coated 12 well plates at 200,000 cells per well in culture media. The cells were exposed to the test compounds **20o** or others (0.3 μM or 1 μM) for 1 h, and EP2 selective agonist ONO-AE1-259-01 (30 nM) for an additional hour and subsequently LPS (100 ng/mL) for 2 h. All compounds were dissolved in DMSO and diluted in media just prior to cell treatment. Following incubation, media was removed from the wells and the cells were subjected to RNA extraction and purification using Trizol and the Zymo Research Quick-RNA miniprep kit according to the manufacturer's protocol (Genesee Scientific). First-strand cDNA synthesis, qRT-PCR and analysis was performed using the primers. Glyceraldehyde-3-phosphate dehydrogenase (GAPDH) was used as a single internal control for relative quantification to determine whether EP2 activation modulates expression of inflammatory mediators in BV2-hEP2 microglia (**Figure 5, 6**). PCR gene expression data are presented as the mean fold change of each gene of interest in the compound treated groups compared to vehicle.

ASSOCIATED CONTENT

Supporting Information

The scanned NMR spectra of all the new compounds and HPLC spectra of key compounds. The Supporting Information is available free of charge on the ACS publications website. This material is available free of charge via the Internet at http://pubs.acs.org.

AUTHOR INFORMATION

Corresponding author

* Email: tganesh@emory.edu; Phone: +1-404-727-7393; Fax: +1-404-727-0365.

Author contributions:

TG designed the overall research. RA and AB and RD participated in research design. TG, RA, SM, DM and VP contributed to synthesis design and performed the synthesis. TG, AB, WW, AR performed bioassays. TG, AB, RD performed data analysis. TG wrote the manuscript. All others contributed to the writing/editing of the manuscript.

ORCID:

Radhika Amaradhi: 0000-0003-0741-4241

Avijit Banik: 0000-0003-3407-3438

Shabber Mohammed: 0000-0002-4852-0596

Vidyavathi Patro: 0000-0002-7107-4870

Asheebo Rojas: 0000-0003-0895-0839

Wenyi Wang: 0000-0001-7148-1700

Damoder Reddy Motati: 0000-0002-4000-1548

Ray Dingledine: 0000-0001-7128-4520

Thota Ganesh: 0000-0002-6163-5590

ACKNOWLEDGEMENTS

This work was supported by NIH/NIA grant U01 AG052460 (T.G.), NINDS grants, R21 NS101167 (T.G.) R01 NS097776 (R.D.), and by ADDF grant 20131001 (T.G.). We also thank ONO Pharmaceutical Co (Osaka, Japan) for providing ONO-AE1-259-01.

ABBREVATIONS USED:

AD, Alzheimer's disease; CNS, central nervous system; PD, Parkinson's disease; SE, status epilepticus; TBI, traumatic brain injury; COX-2, cyclooxygenase-2; HTS, high-throughput screening; EDCI.HCl, 1-ethyl-3-(3-dimethylaminopropyl)carbodiimide .hydrochloride; DMAP, 4-(dimethylamino)pyridine; SAR, Structure activity relationship; MLM, mouse liver microsomes; MPO, multi-parameter optimization; CSF, Cerebrospinal fluid.

REFERENCES

1. Heneka, M. T.; Carson, M. J.; El Khoury, J.; Landreth, G. E.; Brosseron, F.; Feinstein, D. L.; Jacobs, A. H.; Wyss-Coray, T.; Vitorica, J.; Ransohoff, R. M.; Herrup, K.; Frautschy, S. A.; Finsen, B.; Brown, G. C.; Verkhratsky, A.; Yamanaka, K.; Koistinaho, J.; Latz, E.; Halle, A.; Petzold, G. C.; Town, T.; Morgan, D.; Shinohara, M. L.; Perry, V. H.; Holmes, C.; Bazan, N. G.; Brooks, D. J.; Hunot, S.; Joseph, B.; Deigendesch, N.; Garaschuk, O.; Boddeke, E.; Dinarello, C. A.; Breitner, J. C.; Cole, G. M.; Golenbock, D. T.; Kummer, M. P. Neuroinflammation in Alzheimer's Disease. *Lancet Neurol* **2015**, *14*, 388-405.
2. Hirsch, E. C.; Vyas, S.; Hunot, S. Neuroinflammation in Parkinson's Disease. *Parkinsonism Relat Disord* **2012**, *18 Suppl 1*, S210-212.
3. Minghetti, L. Role of Inflammation in Neurodegenerative Diseases. *Curr. Opin. Neurol.* **2005**, *18*, 315-321.

4. Vezzani, A.; French, J.; Bartfai, T.; Baram, T. Z. The Role of Inflammation in Epilepsy. *Nat. Rev. Neurol.* **2011**, *7*, 31-40.

5. Niesman, I. R.; Schilling, J. M.; Shapiro, L. A.; Kellerhals, S. E.; Bonds, J. A.; Kleschevnikov, A. M.; Cui, W.; Voong, A.; Krajewski, S.; Ali, S. S.; Roth, D. M.; Patel, H. H.; Patel, P. M.; Head, B. P. Traumatic Brain Injury Enhances Neuroinflammation and Lesion Volume in Caveolin Deficient Mice. *J. Neuroinflammation* **2014**, *11*, 39-52.

6. Vezzani, A.; Friedman, A.; Dingledine, R. J. The Role of Inflammation in Epileptogenesis. *Neuropharmacology* **2013**, *69*, 16-24.

7. Block, M. L.; Zecca, L.; Hong, J. S. Microglia-Mediated Neurotoxicity: Uncovering the Molecular Mechanisms. *Nat. Rev. Neurosci.* **2007**, *8*, 57-69.

8. Vliet, E. A. V.; Aronica, E.; Vezzani, A.; Ravizza, T. Review: Neuroinflammatory Pathways as Treatment Targets and Biomarker Candidates in Epilepsy: Emerging Evidence from Preclinical and Clinical Studies. *Neuropathol Appl Neurobiol* **2018**, *44*, 91-111.

9. Krstic, D.; Knuesel, I. Deciphering the Mechanism Underlying Late-Onset Alzheimer Disease. *Nat. Rev. Neurol.* **2013**, *9*, 25-34.

10. Ho, L.; Pieroni, C.; Winger, D.; Purohit, D. P.; Aisen, P. S.; Pasinetti, G. M. Regional Distribution of Cyclooxygenase-2 in the Hippocampal Formation in Alzheimer's Disease. *J. Neurosci. Res.* **1999**, *57*, 295-303.

11. Hoozemans, J. J.; van Haastert, E. S.; Veerhuis, R.; Arendt, T.; Scheper, W.; Eikelenboom, P.; Rozemuller, A. J. Maximal Cox-2 and Pprb Expression in Neurons Occurs During Early Braak Stages Prior to the Maximal Activation of Astrocytes and Microglia in Alzheimer's Disease. *J. Neuroinflammation* **2005**, *2*, 27-31.

12. Pasinetti, G. M.; Aisen, P. S. Cyclooxygenase-2 Expression is Increased in Frontal Cortex of Alzheimer's Disease Brain. *Neuroscience* **1998**, *87*, 319-324.

13. Aisen, P. S.; Schafer, K. A.; Grundman, M.; Pfeiffer, E.; Sano, M.; Davis, K. L.; Farlow, M. R.; Jin, S.; Thomas, R. G.; Thal, L. J.; Alzheimer's Disease Cooperative, S. Effects of Rofecoxib or Naproxen Vs Placebo on Alzheimer Disease Progression: A Randomized Controlled Trial. *JAMA* **2003**, *289*, 2819-2826.

14. Arehart, E.; Stitham, J.; Asselbergs, F. W.; Douville, K.; MacKenzie, T.; Fetalvero, K. M.; Gleim, S.; Kasza, Z.; Rao, Y.; Martel, L.; Segel, S.; Robb, J.; Kaplan, A.; Simons, M.; Powell, R. J.; Moore, J. H.; Rimm, E. B.; Martin, K. A.; Hwa, J. Acceleration of Cardiovascular Disease by a Dysfunctional Prostacyclin Receptor Mutation: Potential Implications for Cyclooxygenase-2 Inhibition. *Circ. Res.* **2008**, *102*, 986-993.

15. Egan, K. M.; Lawson, J. A.; Fries, S.; Koller, B.; Rader, D. J.; Smyth, E. M.; Fitzgerald, G. A. Cox-2-Derived Prostacyclin Confers Atheroprotection on Female Mice. *Science* **2004**, *306*, 1954-1957.

16. Grosser, T.; Yu, Y.; Fitzgerald, G. A. Emotion Recollected in Tranquility: Lessons Learned from the Cox-2 Saga. *Annu. Rev. Med.* **2010**, *61*, 17-33.

17. Ganesh, T. Prostanoid Receptor EP2 as a Therapeutic Target. *J. Med. Chem.* **2014**, *57*, 4454-4465.

18. Jiang, J.; Dingledine, R. Prostaglandin Receptor EP2 in the Crosshairs of Anti-Inflammation, Anti-Cancer, and Neuroprotection. *Trends Pharmacol. Sci.* **2013**, *34*, 413-423.

19. Jiang, J.; Quan, Y.; Ganesh, T.; Pouliot, W. A.; Dudek, F. E.; Dingledine, R. Inhibition of the Prostaglandin Receptor EP2 Following Status Epilepticus Reduces Delayed Mortality and Brain Inflammation. *Proc. Natl. Acad. Sci. U.S.A.* **2013**, *110*, 3591-3596.

20. Serrano, G. E.; Lelutiu, N.; Rojas, A.; Cochi, S.; Shaw, R.; Makinson, C. D.; Wang, D.; FitzGerald, G. A.; Dingledine, R. Ablation of Cyclooxygenase-2 in Forebrain Neurons is Neuroprotective and Dampens Brain Inflammation after Status Epilepticus. *J. Neurosci.* **2011**, *31*, 14850-14860.

21. Liang, X.; Wang, Q.; Hand, T.; Wu, L.; Breyer, R. M.; Montine, T. J.; Andreasson, K. Deletion of the Prostaglandin E2 EP2 Receptor Reduces Oxidative Damage and Amyloid Burden in a Model of Alzheimer's Disease. *J. Neurosci.* **2005**, *25*, 10180-10187.

22. Jin, J.; Shie, F. S.; Liu, J.; Wang, Y.; Davis, J.; Schantz, A. M.; Montine, K. S.; Montine, T. J.; Zhang, J. Prostaglandin E2 Receptor Subtype 2 (EP2) Regulates Microglial Activation and Associated Neurotoxicity Induced by Aggregated Alpha-Synuclein. *J. Neuroinflammation* **2007**, *4*, 2-11.

23. Liang, X.; Wang, Q.; Shi, J.; Lokteva, L.; Breyer, R. M.; Montine, T. J.; Andreasson, K. The Prostaglandin E2 EP2 Receptor Accelerates Disease Progression and Inflammation in a Model of Amyotrophic Lateral Sclerosis. *Ann. Neurol.* **2008**, *64*, 304-314.

24. Liu, Q.; Liang, X.; Wang, Q.; Wilson, E. N.; Lam, R.; Wang, J.; Kong, W.; Tsai, C.; Pan, T.; Larkin, P. B.; Shamloo, M.; Andreasson, K. I. PGE2 Signaling via the Neuronal EP2 Receptor Increases Injury in a Model of Cerebral Ischemia. *Proc. Natl. Acad. Sci. U.S.A.* **2019**, *116*, 10019-10024.

25. Montine, T. J.; Milatovic, D.; Gupta, R. C.; Valyi-Nagy, T.; Morrow, J. D.; Breyer, R. M. Neuronal Oxidative Damage from Activated Innate Immunity is EP2 Receptor-Dependent. *J. Neurochem.* **2002**, *83*, 463-470.

26. Rojas, A.; Ganesh, T.; Lelutiu, N.; Gueorguieva, P.; Dingledine, R. Inhibition of the Prostaglandin EP2 Receptor is Neuroprotective and Accelerates Functional Recovery in a Rat Model of Organophosphorus Induced Status Epilepticus. *Neuropharmacology* **2015**, *93*, 15-27.

27. Rojas, A.; Ganesh, T.; Manji, Z.; O'Neill, T.; Dingledine, R. Inhibition of the Prostaglandin E2 Receptor EP2 Prevents Status Epilepticus-Induced Deficits in the Novel Object Recognition Task in Rats. *Neuropharmacology* **2016**, *110*, 419-430.

28. Shie, F. S.; Breyer, R. M.; Montine, T. J. Microglia Lacking E Prostanoid Receptor Subtype 2 Have Enhanced Abeta Phagocytosis yet Lack Abeta-Activated Neurotoxicity. *Am. J. Pathol.* **2005**, *166*, 1163-1172.

29. Forselles, K. J. A.; Root, J.; Clarke, T.; Davey, D.; Aughton, K.; Dack, K.; Pullen, N. In vitro and in vivo Characterization of Pf-04418948, a Novel, Potent and Selective Prostaglandin EP(2) Receptor Antagonist. *Br. J. Pharmacol.* **2011**, *164*, 1847-1856.

30. Jiang, J.; Ganesh, T.; Du, Y.; Quan, Y.; Serrano, G.; Qui, M.; Speigel, I.; Rojas, A.; Lelutiu, N.; Dingledine, R. Small Molecule Antagonist Reveals Seizure-Induced Mediation of Neuronal Injury by Prostaglandin E2 Receptor Subtype EP2. *Proc. Natl. Acad. Sci. U.S.A.* **2012**, *109*, 3149-3154.

31. Ganesh, T.; Jiang, J.; Shashidharamurthy, R.; Dingledine, R. Discovery and Characterization of Carbamothioylacrylamides as EP2 Selective Antagonists. *ACS Med. Chem. Lett.* **2013**, *4*, 616-621.

32. Fox, B. M.; Beck, H. P.; Roveto, P. M.; Kayser, F.; Cheng, Q.; Dou, H.; Williamson, T.; Treanor, J.; Liu, H.; Jin, L.; Xu, G.; Ma, J.; Wang, S.; Olson, S. H. A Selective Prostaglandin E2 Receptor Subtype 2 (EP2) Antagonist Increases the Macrophage-Mediated Clearance of Amyloid-Beta Plaques. *J. Med. Chem.* **2015**, *58*, 5256-5273.

33. Ganesh, T.; Jiang, J.; Yang, M. S.; Dingledine, R. Lead Optimization Studies of Cinnamic Amide EP2 Antagonists. *J. Med. Chem.* **2014**, *57*, 4173-4184.

34. Ganesh, T.; Jiang, J.; Dingledine, R. Development of Second Generation EP2 Antagonists with High Selectivity. *Eur. J. Med. Chem.* **2014**, *82*, 521-535.

35. Ganesh, T.; Banik, A.; Dingledine, R.; Wang, W.; Amaradhi, R. Peripherally Restricted, Highly Potent, Selective, Aqueous-Soluble EP2 Antagonist with Anti-Inflammatory Properties. *Mol. Pharm.* **2018**, *15*, 5809-5817.

36. Salikov, R. F.; Belyy, A. Y.; Khusnutdinova, N. S.; Vakhitova, Y. V.; Tomilov, Y. V. Synthesis and Cytotoxic Properties of Tryptamine Derivatives. *Bioorg. Med. Chem. Lett.* **2015**, *25*, 3597-3600.

37. Salikov, R. F.; Trainov, K. P.; Levina, A. A.; Belousova, I. K.; Medvedev, M. G.; Tomilov, Y. V. Synthesis of Branched Tryptamines via the Domino Cloke-Stevens/Grandberg Rearrangement. *J. Org. Chem.* **2017**, *82*, 790-795.

38. Shmatova, O. I.; Shevchenko, N. E.; Nenajdenko, V. G. Fischer Reaction with 2-Perfluoroalkylated Cyclic Imines ? An Efficient Route to 2-Perfluoroalkyl-Substituted Tryptamines and Their Derivatives and Homologues. *Eur. J. Org. Chem.* **2015**, 6479-6488.

39. Shultz, M. D.; Cao, X.; Chen, C. H.; Cho, Y. S.; Davis, N. R.; Eckman, J.; Fan, J.; Fekete, A.; Firestone, B.; Flynn, J.; Green, J.; Growney, J. D.; Holmqvist, M.; Hsu, M.; Jansson, D.; Jiang, L.; Kwon, P.; Liu, G.; Lombardo, F.; Lu, Q.; Majumdar, D.; Meta, C.; Perez, L.; Pu, M.; Ramsey, T.; Remiszewski, S.; Skolnik, S.; Traebert, M.; Urban, L.; Uttamsingh, V.; Wang, P.; Whitebread, S.; Whitehead, L.; Yan-Neale, Y.; Yao, Y. M.; Zhou, L.; Atadja, P. Optimization of the in vitro Cardiac Safety of Hydroxamate-Based Histone Deacetylase Inhibitors. *J. Med. Chem.* **2011**, *54*, 4752-4772.

40. Pennington, L. D.; Moustakas, D. T. The Necessary Nitrogen Atom: A Versatile High-Impact Design Element for Multiparameter Optimization. *J. Med. Chem.* **2017**, *60*, 3552-3579.

41. Hitchcock, S. A.; Pennington, L. D. Structure-Brain Exposure Relationships. *J. Med. Chem.* **2006**, *49*, 7559-7583.

42. Rankovic, Z. CNS Drug Design: Balancing Physicochemical Properties for Optimal Brain Exposure. *J. Med. Chem.* **2015**, *58*, 2584-2608.

43. Wager, T. T.; Chandrasekaran, R. Y.; Hou, X.; Troutman, M. D.; Verhoest, P. R.; Villalobos, A.; Will, Y. Defining Desirable Central Nervous System Drug Space through the Alignment of Molecular Properties, in vitro ADME, and Safety Attributes. *ACS Chem. Neurosci.* **2010**, *1*, 420-434.

44. Desai, P. V.; Raub, T. J.; Blanco, M.-J. How Hydrogen Bonds Impact P-Glycoprotein Transport and Permeability. *Bioorg. Med. Chem. Lett.* **2012**, *22*, 6540-6548.

45. Herr, R. J. 5-Substituted-1h-Tetrazoles as Carboxylic Acid Isosteres: Medicinal Chemistry and Synthetic Methods. *Bioorg. Med. Chem.* **2002**, *10*, 3379-3393.

46. Bevan, C. D.; Lloyd, R. S. A High-Throughput Screening Method for the Determination of Aqueous Drug Solubility Using Laser Nephelometry in Microtiter Plates. *Anal. Chem.* **2000**, *72*, 1781-1787.

47. Di, L.; Fish, P. V.; Mano, T. Bridging Solubility between Drug Discovery and Development. *Drug Discov. Today* **2012**, *17*, 486-495.

48. Baka, E.; Comer, J. E.; Takacs-Novak, K. Study of Equilibrium Solubility Measurement by Saturation Shake-Flask Method Using Hydrochlorothiazide as Model Compound. *J. Pharm. Biomed. Anal.* **2008**, *46*, 335-341.

49. Sugimoto, Y.; Narumiya, S. Prostaglandin E Receptors. *J. Biol. Chem.* **2007**, *282*, 11613-11617.

50. Wager, T. T.; Hou, X.; Verhoest, P. R.; Villalobos, A. Moving Beyond Rules: The Development of a Central Nervous System Multiparameter Optimization (CNS MPO) Approach to Enable Alignment of Druglike Properties. *ACS Chem. Neurosci.* **2010**, *1*, 435-449.

51. Greaves, E.; Horne, A. W.; Jerina, H.; Mikolajczak, M.; Hilferty, L.; Mitchell, R.; Fleetwood-Walker, S. M.; Saunders, P. T. EP2 Receptor Antagonism Reduces Peripheral and Central Hyperalgesia in a Preclinical Mouse Model of Endometriosis. *Sci. Rep.* **2017**, *7*, 44169-44178.

52. Sheibanie, A. F.; Khayrullina, T.; Safadi, F. F.; Ganea, D. Prostaglandin E2 Exacerbates Collagen-Induced Arthritis in Mice through the Inflammatory Interleukin-23/Interleukin-17 Axis. *Arthritis Rheumatol.* **2007**, *56*, 2608-2619.

53. Sheibanie, A. F.; Yen, J. H.; Khayrullina, T.; Emig, F.; Zhang, M.; Tuma, R.; Ganea, D. The Proinflammatory Effect of Prostaglandin E2 in Experimental Inflammatory Bowel Disease is Mediated through the Il-23-->Il-17 Axis. *J. Immunol.* **2007**, *178*, 8138-8147.

54. Rojas, A.; Banik, A.; Chen, D.; Flood, K.; Ganesh, T.; Dingledine, R. Novel Microglia Cell Line Expressing the Human EP2 Receptor. *ACS Chem. Neurosci.* **2019**, *10*, 4280-4292.

55. Quan, Y.; Jiang, J.; Dingledine, R. EP2 Receptor Signaling Pathways Regulate Classical Activation of Microglia. *J. Biol. Chem.* **2013**, *288*, 9293-9302.

56. Jiang, J.; Dingledine, R. Role of Prostaglandin Receptor EP2 in the Regulations of Cancer Cell Proliferation, Invasion, and Inflammation. *J. Pharmacol. Exp. Ther.* **2013**, *344*, 360-367.

57. Salikov, R. F.; Trainov, K. P.; Belousova, I. K.; Belyy, A. Y.; Fatkullina, U. S.; Mulyukova, R. V.; Zainullina, L. F.; Vakhitova, Y. V.; Tomilov, Y. V. Branching Tryptamines as a Tool to Tune Their Antiproliferative Activity. *Eur. J. Med. Chem.* **2018**, *144*, 211-217.

58. Baggett, A. W.; Cournia, Z.; Han, M. S.; Patargias, G.; Glass, A. C.; Liu, S.-Y.; Nolen, B. J. Structural Characterization and Computer-Aided Optimization of a Small-Molecule Inhibitor of

the Arp2/3 Complex, a Key Regulator of the Actin Cytoskeleton. *ChemMedChem* **2012**, *7*, 1286-1294.

59. Liang, X.-W.; Liu, C.; Zhang, W.; You, S.-L. Asymmetric Fluorinative Dearomatization of Tryptamine Derivatives. *ChemComm* **2017**, *53*, 5531-5534.
60. Shevchenko, N. E.; Balenkova, E. S.; Röschenthaler, G.-V.; Nenajdenko, V. G. Practical Synthesis of A-Perfluoroalkyl Cyclic Imines and Amines. *Synthesis* **2010**, 120-126.
61. Shmatova, O. I.; Shevchenko, N. E.; Nenajdenko, V. G. Fischer Reaction with 2-Perfluoroalkylated Cyclic Imines — an Efficient Route to 2-Perfluoroalkyl-Substituted Tryptamines and Their Derivatives and Homologues. *Eur. J. Org. Chem.* **2015**, 6479-6488.
62. Shultz, M. D.; Cao, X.; Chen, C. H.; Cho, Y. S.; Davis, N. R.; Eckman, J.; Fan, J.; Fekete, A.; Firestone, B.; Flynn, J.; Green, J.; Growney, J. D.; Holmqvist, M.; Hsu, M.; Jansson, D.; Jiang, L.; Kwon, P.; Liu, G.; Lombardo, F.; Lu, Q.; Majumdar, D.; Meta, C.; Perez, L.; Pu, M.; Ramsey, T.; Remiszewski, S.; Skolnik, S.; Traebert, M.; Urban, L.; Uttamsingh, V.; Wang, P.; Whitebread, S.; Whitehead, L.; Yan-Neale, Y.; Yao, Y.-M.; Zhou, L.; Atadja, P. Optimization of the in vitro Cardiac Safety of Hydroxamate-Based Histone Deacetylase Inhibitors. *J. Med. Chem.* **2011**, *54*, 4752-4772.
63. Sum, P.-E.; How, D. B.; Sabatini, J. J.; Xiang, J. S.; Ipek, M.; Feyfant, E. Preparation of Glutamate Derivatives as Aggrecanase Inhibitors. WO2007008994A2, 2007.
64. Blake, T. D.; Hamper, B. C.; Huang, W.; Kiefer, J. R.; Moon, J. B.; Neal, B. E.; Olson, K. L.; Pelc, M. J.; Schweitzer, B. A.; Thorarensen, A.; Trujillo, J. I.; Turner, S. R. Preparation of Nicotinamide Derivatives as H-Pgds (Hematopoietic Prostaglandin D Synthase) Inhibitors. US20080146569A1, 2008.

65. Westaway, S. M.; Thompson, M.; Rami, H. K.; Stemp, G.; Trouw, L. S.; Mitchell, D. J.; Seal, J. T.; Medhurst, S. J.; Lappin, S. C.; Biggs, J.; Wright, J.; Arpino, S.; Jerman, J. C.; Cryan, J. E.; Holland, V.; Winborn, K. Y.; Coleman, T.; Stevens, A. J.; Davis, J. B.; Gunthorpe, M. J. Design and Synthesis of 6-Phenylnicotinamide Derivatives as Antagonists of Trpv1. *Bioorg. Med. Chem. Lett.* **2008**, *18*, 5609-5613.

66. Bentzien, J. M.; Boyer, S. J.; Burke, J.; Eldrup, A. B.; Guo, X.; Huber, J. D.; Kirrane, T. M.; Soleymanzadeh, F.; Swinamer, A. D. Pyrrolidinyl and Piperidinyl Compounds Useful as Nhe-1 Inhibitors and Their Preparation and Pharmaceutical Compositions. WO2010005783A1, 2010.

67. Fandrick, D. R.; Reinhardt, D.; Desrosiers, J.-N.; Sanyal, S.; Fandrick, K. R.; Ma, S.; Grinberg, N.; Lee, H.; Song, J. J.; Senanayake, C. H. General and Rapid Pyrimidine Condensation by Addressing the Rate Limiting Aromatization. *Org. Lett.* **2014**, *16*, 2834-2837.

68. Juby, P. F.; Hudyma, T. W.; Brown, M.; Essery, J. M.; Partyka, R. A. Antiallergy Agents. 2. 2-Phenyl-5-(1*H*-tetrazol-5-yl)pyrimidin-4(3*H*)-ones. *J. Med. Chem.* **1982**, *25*, 1145-1150.

69. Ricci, P.; Kramer, K.; Cambeiro, X. C.; Larrosa, I. Arene-metal Π-complexation as a Traceless Reactivity Enhancer for C-H Arylation. *J. Am. Chem. Soc.* **2013**, *135*, 13258-13261.

70. Senaweera, S.; Weaver, J. D. Dual C-F, C-H Functionalization via Photocatalysis: Access to Multifluorinated Biaryls. *J. Am. Chem. Soc.* **2016**, *138*, 2520-2523.

71. Shen, Y.; Wu, X.-X.; Chen, S.; Xia, Y.; Liang, Y.-M. Synthesis of Polyfluoroarene-Substituted Benzofuran Derivatives via Cooperative Pd/Cu Catalysis. *ChemComm* **2018**, *54*, 2256-2259.

72. Hansen, A. H.; Sergeev, E.; Bolognini, D.; Sprenger, R. R.; Ekberg, J. H.; Ejsing, C. S.; McKenzie, C. J.; Rexen Ulven, E.; Milligan, G.; Ulven, T. Discovery of a Potent Thiazolidine Free Fatty Acid Receptor 2 Agonist with Favorable Pharmacokinetic Properties. *J. Med. Chem.* **2018**, *61*, 9534-9550.

73. Jiang, J.; Ganesh, T.; Du, Y.; Thepchatri, P.; Rojas, A.; Lewis, I.; Kurtkaya, S.; Li, L.; Qui, M.; Serrano, G.; Shaw, R.; Sun, A.; Dingledine, R. Neuroprotection by Selective Allosteric Potentiators of the EP2 Prostaglandin Receptor. *Proc. Natl. Acad. Sci. U.S.A.* **2010**, *107*, 2307-2312.

TOC (graphical)